WORKING PAPER

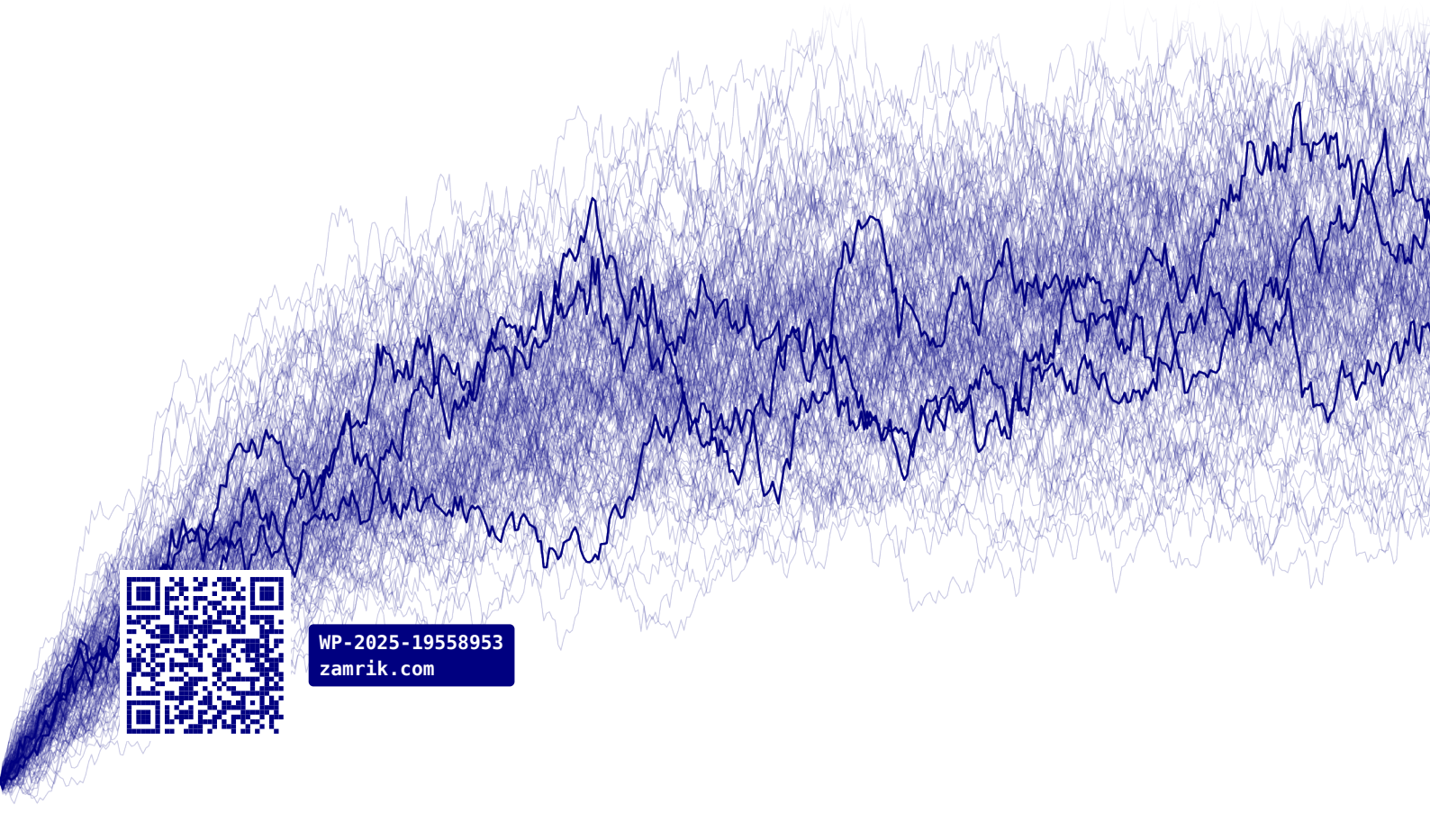
The Joint Law of the Times of the Maxima of Correlated Brownian Motions

Wedge Kernels, a Chaos Expansion and Correlated Bridges

Supervised by Dr. T. Zamrik

24-JUN-2025

Sample paths of the Cox–Ingersoll–Ross process: $dX_t = \kappa(\theta - X_t)\,dt + \sigma\sqrt{X_t}\,dW_t, \quad \kappa = 3.87,\ \theta = 1.10,\ \sigma = 0.53,\ X_0 = 0.22$



WP-2025-19558953
zamrik.com



Zamrik Quant Research

The research arm of Zamrik Quant Lab

Copyright

© 2025 T. Zamrik. All rights reserved. Published by Zamrik Quant Research. No part of this document may be reproduced, stored, distributed or adapted, in whole or in part, by any means, without the prior written permission of the publisher, except for brief quotation with full citation. Requests for permission: info@zamrik.com.

Suggested Citation

Stochastic Analysis Desk, Zamrik Quant Research (2025). 'The Joint Law of the Times of the Maxima of Correlated Brownian Motions: Wedge Kernels, a Chaos Expansion and Correlated Bridges'. *Zamrik Quant Research Working Paper* **WP-2025-19558953**. Available at https://zamrik.com/research-items/wp-2025-19558953/.

About Zamrik Quant Research

Zamrik Quant Research is the research arm of Zamrik Quant Lab. It works through five research desks, from market microstructure and derivatives to optimal control, stochastic analysis and applied mathematics, and publishes everything it finds in the open: research papers, notebooks that run on Kaggle, free tools that answer one practical question, and essays.

The five desks are Market Microstructure & Trading; Derivatives & Volatility; Optimal Control & Decision; Stochastic Analysis; and Applied Mathematics. Each paper, notebook, tool and essay belongs to exactly one desk. Zamrik Quant Research is run by a small, independent team, headed by Dr. T. Zamrik. We are self-funded: no sponsors, no advertisers, no outside capital.

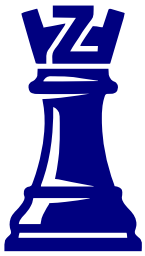
Every publication passes through the same five functions before anyone outside sees it: research, data, software, verification and production. We never retrofit the mathematics to a conclusion chosen in advance. Every number is checked two independent ways. Every figure is re-run from its code. When we find an error, or replace a piece with a better one, we record it in the public corrections log at https://zamrik.com/corrections/.

Legal Notice

This paper is research and education. Nothing in it is investment, financial, legal or engineering advice; nothing is a recommendation to buy or sell shares of stock, derivative contracts, bonds, or any other instrument or property; and nothing is a forecast. You are responsible for your own decisions. Figures and code are provided as they are. Care and independent checks reduce errors but cannot rule them out, so no warranty is given. The views expressed are those of the Stochastic Analysis Desk.

STOCHASTIC ANALYSIS DESK ZAMRIK QUANT RESEARCH

WORKING PAPER



The Joint Law of the Times of the Maxima of Correlated Brownian Motions

Wedge Kernels, a Chaos Expansion and Correlated Bridges

Supervised by Dr. T. Zamrik[1]

24-JUN-2025 WP-2025-19558953

Abstract. Let W_1 and W_2 be standard Brownian motions on $[0,1]$ with correlation ρ, and θ_1, θ_2 the times of their maxima. Rogers and Shepp found the correlation of the two maximum values; we study the two times. As one planar path, the pair stays in the wedge with apex (M_1, M_2) and angle $\alpha = \arccos(-\rho)$ and touches its two edges at θ_1 and θ_2. Cutting the path at the touches gives the joint density of (θ_1, θ_2) as a double integral of two Bessel series of the wedge heat kernel, and the probability that both maxima occur before t exactly through two independent copies of (M_1, M_2). Near the diagonal the density behaves like $|t-s|^{\pi/\alpha-2}$: the times repel for $\rho < 0$ and attract for $\rho > 0$, the argmax counterpart of a dichotomy for first-passage times. The correlation of the times is $\sum_n c_n \rho^n$ with $c_n \geq 0$, $\sum_n c_n = 1$ and $\sum_n (-1)^n c_n = (6 - 7\zeta(3))/4$, the value of Mori, Majumdar and Schehr at $\rho = -1$, and exactly $c_1 = 4 - 32/(3\pi)$, which gives two-sided bounds; the correlation itself has no closed form. At $\alpha = \pi/n$ the kernels are finite image sums. For correlated bridges θ_1 is uniform and independent of the cyclic gap, whose density is elementary at $\alpha = \pi/n$. Quadrature, 12 million simulated pairs, several motions and four laws of random-walk steps support and extend the results.

WP-2025-19558953 · Stochastic Analysis Desk · Working Paper · Published 24-JUN-2025 · Reading time: about 40 min

1. Introduction

A standard Brownian motion on $[0,1]$ reaches its maximum M at one time θ, which follows the arcsine law. The joint density of (M, θ) is classical [1]; near its maximum the path splits into two independent meanders [2]; and the time of the maximum is known for many constrained motions [3].

For two motions with correlation ρ, the law of the maximum values (M_1, M_2) has a long history: Rogers and Shepp [4] computed $E[M_1 M_2]$ as a single integral, Iyengar [5] found the joint law from the hitting distribution of planar Brownian motion on two lines, Shao and Wang [6] bounded it, and Dębicki, Ji and Rolski [7] found the tail asymptotics of the suprema with drift. Behind all of these is one picture: the pair is a linear image of planar Brownian motion, $\{M_1 < a_1, M_2 < a_2\}$ asks the planar path to stay in a wedge,

[1]Correspondence: Stochastic Analysis Desk, Zamrik Quant Research, info@zamrik.com.

and the wedge has an explicit heat kernel [8], [9]; the same picture gives first-passage laws for correlated motions [10], [11]. We ask the twin question: what is the joint law of the times (θ_1, θ_2), and how does $\operatorname{corr}(\theta_1, \theta_2)$ depend on ρ?

Two endpoints are known. At $\rho = 0$ the times are independent arcsine variables. At $\rho = -1$, θ_2 is the time of the minimum of W_1, and Mori, Majumdar and Schehr [12], [13] found the law of $t_{\min} - t_{\max}$ for Brownian motion and the bridge, with $\operatorname{cov}(t_{\max}, t_{\min}) = -(7\zeta(3) - 6)/32$ and $-(\pi^2 - 9)/36$. Hartmann and Majumdar [14] found pairwise joint laws of three characteristic times of one motion. Houdré and Litherland [15] studied a different generalization of the arcsine law, the maximizing chain of times of one functional of independent motions, whose chamber is one of times, not of space.

The closest method is that of Kou and Zhong [11], who used the same wedge for the first-passage times of a correlated pair and proved that the density of their difference blows up at 0 if and only if $\rho > 0$; the same sign decides whether a reflected motion visits the corner of the wedge [16]. The persistence exponent $\pi/(2\alpha)$ of walks in a wedge is that of Denisov and Wachtel [17], and Gebelein's inequality [18] bounds the correlation of functions of a Gaussian pair by $|\rho|$. To our knowledge, the joint law of the times of the maxima of correlated Brownian motions has not appeared: the works citing [4] that we found, and those above, treat the values, the times of one path, or first-passage times.

The planar path stays in the wedge with apex at (M_1, M_2) and touches its two edges exactly at θ_1 and θ_2. Cutting it at the two touches leaves three pieces, a first exit, an edge-to-edge passage and a survival, whose laws are given by the Dirichlet heat kernel of the wedge. Section 2 proves the decomposition, Section 3 gives the joint density, Section 4 the local exponents, Section 5 the correlation, Section 6 the wedges of angle π/n, Section 7 correlated bridges, Sections 8 and 9 several motions and random walks (numerically), and Section 10 what is not proved.

Main findings

- For two standard Brownian motions with correlation ρ, the joint density of the times of their maxima is $f_\rho(s,t) = (\sin\alpha/4) \iint D_s(r_1) K_{t-s}(r_1, r_2) D_{1-t}(r_2)\, dr_1\, dr_2$ for $s < t$, where $\alpha = \arccos(-\rho)$ is the angle of the wedge $\{W_1 < M_1, W_2 < M_2\}$, D the normal derivative of its survival function and K the edge-to-edge derivative of its heat kernel; it reproduces the arcsine marginals to 7.7×10^{-11} and Rogers and Shepp's $E[M_1 M_2]$ to 4.1×10^{-13}, and agrees with 12 million simulated pairs (Theorem 1, Corollary 1).

- Near the diagonal $f_\rho(s, s+u) \sim C(s)\, u^{\pi/\alpha - 2}$: the two times repel each other for $\rho < 0$, where the density of $|\theta_1 - \theta_2|$ vanishes like $u^{\pi/(2\alpha)-1}$ because near-coincidences occur only at the ends of $[0,1]$, and attract each other for $\rho > 0$, where it blows up like $u^{\pi/\alpha - 2}$; at $\rho = 0$ it diverges only like $(4/\pi^2)\log(1/u)$, and $P(\theta_1 \le \varepsilon, \theta_2 \le \varepsilon) \sim C\varepsilon^{\pi/(2\alpha)}$ (Proposition 2, Corollary 2).

- $\operatorname{corr}(\theta_1, \theta_2) = \sum_{n \ge 1} c_n \rho^n$ with $c_n \ge 0$, $\sum_n c_n = 1$ and $\sum_n (-1)^n c_n = (6 - 7\zeta(3))/4$, and exactly $c_1 = 4 - 32/(3\pi) = 0.60469$, which gives two-sided bounds such as $|\operatorname{corr}(\theta_1, \theta_2)| \le 0.8018\, |\rho|$ for $\rho < 0$ (Theorems 2 and 3, Corollary 3).

- At $\alpha = \pi/n$, that is $\rho = -1/2, -1/\sqrt{2}, -\sqrt{3}/2, \dots$, both kernels are finite image sums of Gaussians and normal distribution functions, and the law of the cyclic gap of correlated bridges is elementary (Theorem 4, Proposition 3).
- For correlated Brownian bridges, θ_1 is uniform and independent of $D = (\theta_2 - \theta_1) \bmod 1$, whose density is $(\pi \sin \alpha/2) \iint K_u K_{1-u}$, and $\operatorname{corr}(\theta_1, \theta_2) = 6 \operatorname{Var} D - 1/2$ (Theorems 5 and 6).
- For random walks the marginal law of the index of the maximum is universal but the joint law of the two indices is not: $P(\vartheta_1 = \vartheta_2 = 0)$ differs between four step laws with the same correlation by up to 93.3 standard errors at $n = 10$, while all four converge to the Brownian correlation (Section 9).

2. The Wedge and the Path Decomposition

Definition 1 (The pair and the times of its maxima)**.** Let $\rho \in (-1, 1)$, $\bar{\rho} = \sqrt{1 - \rho^2}$ and $Z = (X, Y)$ a standard planar Brownian motion on $[0, 1]$. Put $W_1 = X$ and $W_2 = \rho X + \bar{\rho} Y$, standard Brownian motions with $E[W_1(u) W_2(v)] = \rho \min(u, v)$, with maxima M_1, M_2 attained at the times θ_1, θ_2. On $\{\theta_1 < \theta_2\}$ the gaps are $G = M_2 - W_2(\theta_1)$ and $H = M_1 - W_1(\theta_2)$; on $\{\theta_2 < \theta_1\}$ the indices are exchanged.

Each maximum is attained once almost surely [1], and $P(\theta_1 = \theta_2) = 0$ by Corollary 1. The laws depend on the pair only through ρ. At $\rho = 1$, $\theta_1 = \theta_2$; at $\rho = -1$, θ_2 is the time of the minimum of W_1.

Definition 2 (The wedge and its kernels)**.** Let $u_1 = (1, 0)$, $u_2 = (\rho, \bar{\rho})$, so $W_i = \langle u_i, Z \rangle$, and for $a_1, a_2 > 0$ let $C_a = \{z : \langle u_1, z \rangle < a_1,\ \langle u_2, z \rangle < a_2\}$, with edge i on the line $\langle u_i, z \rangle = a_i$. Let $\alpha = \arccos(-\rho)$, $p = \pi/\alpha$, $\nu_n = np$, and (r, φ) polar coordinates about the apex, $\varphi = 0$ on edge 1 and $\varphi = \alpha$ on edge 2. Then $p_t(z, z')$ is the Dirichlet heat kernel of C_a for $\frac{1}{2}\Delta$; $S_t(z) = \int_{C_a} p_t(z, z')\, dz'$ is the probability of staying in C_a up to time t; $D_t(r)$ is the derivative of S_t along the inward normal n_1 at the point P_1 of edge 1 at distance r from the apex; $K_u(r_1, r_2)$ is the mixed derivative of $p_u(z, z')$ along n_1 in z at P_1 (distance r_1) and along the inward normal n_2 of edge 2 in z' at P_2 (distance r_2), written $\partial_{n_1} \partial_{n_2}$; and $\delta = D_1$, $k = K_1$.

All wedges C_a are translates, so the kernels do not depend on a in coordinates about the apex; the reflection in the bisector exchanges the edges, so D_t is the same on both and $K_u(r_1, r_2) = K_u(r_2, r_1)$.

Lemma 1 (The planar path lives in a wedge)**.** $a_i - \langle u_i, z \rangle$ is the signed distance from z to the line of edge i, the interior angle of C_a is $\alpha = \arccos(-\rho)$, and a point of one edge at distance r from the apex is at distance $r \sin \alpha$ from the line of the other. For $b_1, b_2 > 0$,

$$\{M_1 < b_1,\ M_2 < b_2\} = \{Z(t) \in C_b \text{ for all } t \in [0, 1]\};$$

the path stays in the closure of C_M, $M = (M_1, M_2)$, and meets edge i of C_M exactly at θ_i; on $\{\theta_1 < \theta_2\}$ the touching points lie at distances $G/\sin \alpha$ and $H/\sin \alpha$ from the apex.

Proof. $|u_i| = 1$ *gives the distances. The outward normals* u_1, u_2 *satisfy* $\langle u_1, u_2\rangle = \rho$*, so the interior angle is* $\pi - \arccos\rho = \arccos(-\rho)$*. By continuity on* $[0,1]$*,* $M_i < b_i$ *if and only if* $W_i(t) < b_i$ *for all* t*. With* $b = M$*,* $W_i(t) \le M_i$ *with equality only at* θ_i*, the maximum being attained once. At* θ_1 *the distance to the line of edge 2 is* $M_2 - W_2(\theta_1) = G$*, and likewise for* H*.* □

The identity is the starting point of [5] for the law of (M_1, M_2); here we follow the path into the corner.

Lemma 2 (Eigen-series and scaling forms)**.** With I_μ the modified Bessel function of the first kind: (a)

$$p_t(r,\varphi;r',\varphi') = \frac{2}{\alpha t} e^{-(r^2+r'^2)/(2t)} \sum_{n\ge 1} I_{\nu_n}(rr'/t)\sin(\nu_n\varphi)\sin(\nu_n\varphi'),$$

converging with all derivatives uniformly on compact subsets of the closed wedge minus its apex; (b)

$$S_t(r,\varphi) = \sum_{m \text{ odd}} \frac{4}{m\pi}\sin(\nu_m\varphi)\, G_m(r^2/(4t)),$$

with

$$G_m(z) = \sqrt{\pi z/2}\, e^{-z}[I_{(\nu_m-1)/2}(z) + I_{(\nu_m+1)/2}(z)];$$

(c)

$$D_t(r) = \frac{4}{\alpha r}\sum_{m \text{ odd}} G_m(r^2/(4t)) = t^{-1/2}\delta(r/\sqrt{t});$$

(d)

$$\begin{aligned} K_u(r_1,r_2) &= \frac{2}{\alpha u r_1 r_2} e^{-(r_1^2+r_2^2)/(2u)} \sum_{n\ge 1}(-1)^{n+1}\nu_n^2 I_{\nu_n}(r_1 r_2/u) \\ &= u^{-2}k(r_1/\sqrt{u}, r_2/\sqrt{u}); \end{aligned}$$

(e) $\delta(x) = c_\alpha x^{p-1}(1+O(x^2))$ as $x\to 0$ and $k(x,y) = c_k (xy)^{p-1} e^{-(x^2+y^2)/2}(1+O(xy))$ as $xy\to 0$, with

$$c_\alpha = \frac{2}{\alpha}\sqrt{\pi/2}\, 8^{-(p-1)/2}/\Gamma(\frac{p+1}{2})$$

and $c_k = 2p^2/(\alpha 2^p \Gamma(p+1))$; and $S_t(r,\varphi) = (c_\alpha/p)\sin(p\varphi)(r/\sqrt{t})^p(1+o(1))$ as $r/\sqrt{t}\to 0$; (f) at $\rho = 0$, $\delta(x) = \sqrt{2/\pi}\,\operatorname{erf}(x/\sqrt{2})$ and $k(x,y) = (2/\pi)\, xy\, e^{-(x^2+y^2)/2}$.

Proof. is the Dirichlet eigen-expansion of the wedge [8], [9], with angular eigenfunctions $\sin(\nu_n\varphi)$*; by Lemma 3 the n-th term and its derivatives are bounded by a polynomial in* ν_n *times* $(rr'/(2t))^{\nu_n}/\Gamma(\nu_n+1)$ *while* rr'/t *is bounded. (b) Integrate (a) term by term: the angular integral* $\int_0^\alpha \sin(\nu_n\varphi')\,d\varphi'$ *is* $2\alpha/(n\pi)$ *for odd* n *and* 0 *for even* n*, and the radial one is the case* $\mu = 2$ *of Weber's first exponential integral (§13.3 of [25]),*

$$\begin{aligned} \int_0^\infty x e^{-ax^2} I_\nu(bx)\,dx = \frac{\sqrt{\pi}\, b}{8a^{3/2}}\, e^{b^2/(8a)} \Big[& I_{\frac{\nu-1}{2}}\Big(\frac{b^2}{8a}\Big) \\ & + I_{\frac{\nu+1}{2}}\Big(\frac{b^2}{8a}\Big)\Big], \end{aligned}$$

obtained by integrating the power series of I_ν termwise and summing the Kummer series; at $a = 1/(2t)$, $b = r/t$ it is $t\sqrt{\pi z/2}\, e^z[\dots]$, $z = r^2/(4t)$. (c) The inward normal derivative at $\varphi = 0$ is $r^{-1}\partial_\varphi$, and $\partial_\varphi \sin(\nu_m\varphi) = m\pi/\alpha$ there; each term depends on r^2/t only. (d) Apply $r_1^{-1}\partial_\varphi$ at $\varphi = 0$ and $-r_2^{-1}\partial_{\varphi'}$ at $\varphi' = \alpha$, which gives $(-1)^{n+1}\nu_n/r_2$. (e) $I_\mu(z) = (z/2)^\mu\Gamma(\mu+1)^{-1}(1+O(z^2))$; the term $m = 1$ of (c) gives $c_\alpha x^{p-1}$, its next order is smaller by x^2 and the term $m = 3$ by $x^{2p} = o(x^2)$ since $p > 1$; likewise for $n = 1$ in (d) and $m = 1$ in (b). (f) At $\alpha = \pi/2$ the kernel is a product of two half-line kernels; the half-line survival from distance x is $\operatorname{erf}(x/\sqrt{2t})$, with boundary derivative $\sqrt{2/(\pi t)}$, and the boundary derivative of the half-line kernel at y is $2ye^{-y^2/(2t)}/(t\sqrt{2\pi t})$. □

Lemma 3 (A rigorous truncation bound)**.** For $\mu > -1/2$ and $z > 0$, $0 < I_\mu(z)\, e^{-z} \le (z/2)^\mu/\Gamma(\mu+1)$. Hence the series of Lemma 2(d) at $u = 1$, cut after N terms, errs by at most

$$\frac{2}{\alpha xy}\, e^{-(x-y)^2/2} \sum_{n>N} \frac{\nu_n^2 (xy/2)^{\nu_n}}{\Gamma(\nu_n+1)},$$

and the series of Lemma 2(c) by the same bound applied to both Bessel functions of each omitted G_m.

Proof. By Poisson's integral,

$$I_\mu(z) = \frac{(z/2)^\mu}{\sqrt{\pi}\,\Gamma(\mu+\frac12)} \int_{-1}^{1} (1-t^2)^{\mu-1/2} e^{zt}\, dt;$$

bound $e^{zt} \le e^z$ and use

$$\int_{-1}^{1} (1-t^2)^{\mu-1/2} dt = \sqrt{\pi}\,\Gamma(\mu+\frac12)/\Gamma(\mu+1).$$

Then $e^{-(x^2+y^2)/2} I_\nu(xy) \le e^{-(x-y)^2/2}(xy/2)^\nu/\Gamma(\nu+1)$. The orders $(\nu_m \mp 1)/2$ in G_m exceed $-1/2$ because $\nu_m \ge p > 1$. □

The bound decays faster than geometrically and needs no knowledge of the sum, so it serves as a stopping rule. The computations cut both series where it falls below 10^{-16} on the whole quadrature grid; on the five correlations whose cut-offs are reported in the checks, the largest bound on a dropped tail is 4.4×10^{-17}.

Lemma 4 (Gaussian bounds by comparison with a half-plane)**.** Let $g_t(v) = (2\pi t)^{-1} e^{-|v|^2/(2t)}$, $d_i(z)$ the distance from z to the line of edge i, and $q = |P_1 - P_2|^2 = r_1^2 + r_2^2 - 2r_1 r_2 \cos\alpha$. Then: (i) $0 \le \partial_{n_1} p_t(P_1, z) \le (2d_1(z)/t)\, g_t(P_1 - z)$, likewise on edge 2, and $0 \le D_t \le \sqrt{2/(\pi t)}$; (ii) $0 \le K_u(r_1, r_2) \le \frac{8}{\pi u^2}(1 + \frac{q}{2u}) e^{-q/(2u)}$, with $q \ge (1 - |\cos\alpha|)(r_1^2 + r_2^2)$; (iii) for a constant C_α, $\delta(x) \le C_\alpha x^{p-1}$, $k(x,y) \le C_\alpha (xy)^{p-1}$ and $S_1(r,\varphi) \le C_\alpha r^p$; (iv) $\delta(x) \to \sqrt{2/\pi}$ as $x \to \infty$.

Proof. Let $\mathcal{H} \supset C_a$ be the half-plane of edge 1, with kernel $p_t^{\mathcal{H}}(z, z') = g_t(z - z') - g_t(z - \bar{z}')$, $\bar{z}'$ the mirror image. A path killed on leaving C_a dies no later than one killed on leaving $\mathcal{H}$, so $0 \le p_t \le p_t^{\mathcal{H}}$ and $S_t \le S_t^{\mathcal{H}}$. (i) For $z_\varepsilon = P_1 + \varepsilon n_1$, $|z_\varepsilon - \bar{z}|^2 - |z_\varepsilon - z|^2 = 4\varepsilon d_1(z)$,

so

$$\begin{aligned} 0 &\le \varepsilon^{-1} p_t(z_\varepsilon, z) \\ &\le \varepsilon^{-1} g_t(z_\varepsilon - z)(1 - e^{-2\varepsilon d_1(z)/t}) \\ &\le (2d_1(z)/t)\, g_t(z_\varepsilon - z); \end{aligned}$$

let $\varepsilon \to 0$. *The same with* $S_t^{\mathcal{H}}(z) = \operatorname{erf}(d_1(z)/\sqrt{2t})$ *bounds* D_t. *(ii) By Chapman–Kolmogorov,* $p_u(z,z') = \int_{C_a} p_{u/2}(z,w) p_{u/2}(w,z')\, dw$. *The difference quotients are dominated, uniformly in* $\varepsilon \le 1$, *by (i) and* $g_t(z_\varepsilon - w) \le 2e^{1/(2t)} g_{2t}(P_1 - w)$, *so*

$$\begin{aligned} K_u(r_1, r_2) &= \int_{C_a} \partial_{n_1} p_{u/2}(P_1, w)\, \partial_{n_2} p_{u/2}(w, P_2)\, dw \\ &\le \frac{16}{u^2} \int_{\mathbb{R}^2} d_1(w) d_2(w)\, g_{u/2}(P_1 - w)\, g_{u/2}(w - P_2)\, dw. \end{aligned}$$

With $d_i(w) \le |w - P_i|$ *and* $g_{u/2}(P_1 - w) g_{u/2}(w - P_2) = g_u(P_1 - P_2) g_{u/4}(w - m)$, m *the midpoint, the integral is at most* $g_u(P_1 - P_2) E[(|V| + \tfrac{1}{2}|P_1 - P_2|)^2] \le g_u(P_1 - P_2)(u + q/2)$, V *centered Gaussian with covariance* $(u/4)I$. *Also* $2r_1 r_2 |\cos\alpha| \le |\cos\alpha|(r_1^2 + r_2^2)$. *(iii) For* $x \le 1$ *and* $xy \le 1$, *Lemmas 2 and 3 give* $\delta(x) \le C x^{p-1}$ *and*

$$k(x,y) \le \frac{2}{\alpha} (xy)^{p-1} \sum_n \nu_n^2 2^{-\nu_n} / \Gamma(\nu_n + 1);$$

otherwise $\delta \le \sqrt{2/\pi}$ *by (i) and* $k \le 8/\pi$ *by (ii), and* $p > 1$. *For* S_1 *use Lemma 2(b) if* $r \le 1$ *and* $S_1 \le 1$ *if not. (iv)* $S_1^{\mathcal{H}} - S_1$ *is the probability of leaving* C_a *through edge* 2 *before time* 1 *and then surviving in* $\mathcal{H}$*: non-negative, zero on edge* 1, *and at most the exit flux* $\int_0^1 \int_0^\infty \tfrac{1}{2} \partial_{n_2} p_s(\cdot, P_2)\, dr_2\, ds$. *Hence*

$$0 \le \sqrt{2/\pi} - \delta(x) \le \frac{1}{2} \int_0^1 \int_0^\infty K_s(x, r_2)\, dr_2\, ds \to 0$$

by (ii). □

Theorem 1 (The wedge decomposition)**.** Let $\rho \in (-1, 1)$. On $\{\theta_1 < \theta_2\}$ the vector $(\theta_1, \theta_2, M_1, M_2, G, H)$ has the density

$$\frac{1}{4 \sin^2 \alpha}\, \partial_{n_1} p_s(z_a, P_1)\, \partial_{n_1} \partial_{n_2} p_{t-s}(P_1, P_2)\, \partial_{n_2} S_{1-t}(P_2)$$

at (s, t, a_1, a_2, g, h), $0 < s < t < 1$, $a_i, g, h > 0$. The kernels are those of C_a; $z_a = 0$ is the starting point, at distances a_1, a_2 from the edges; P_1 is the point of edge 1 at distance $r_1 = g/\sin\alpha$ from the apex and P_2 that of edge 2 at distance $r_2 = h/\sin\alpha$. On $\{\theta_2 < \theta_1\}$ the edges are exchanged.

Proof. Fix a, $s < t$, g, h; *then* P_1, P_2 *lie away from the apex. Let* $\varepsilon > 0$, $\mathbf{1} = (1,1)$, $e_1 = (1,0)$. *Step 1. The exit time* T *of* Z *from* C_a *and the exit point have the density* $\tfrac{1}{2} \partial_{n_1} p_s(z_a, P_1)$ *per unit time and length of edge* 1 *[8], [9]: the flux of the killed density; the apex is hit with probability zero. Step 2. Let* F_ε *be the event:* Z *leaves* C_a *through edge* 1 *at a time in* ds *and a point in* dP_1*; then stays in* $C_{a+\varepsilon e_1}$ *until it leaves through edge* 2 *at*

a time in dt and a point in dP_2; then stays in $C_{a+\varepsilon\mathbf{1}}$ up to time 1. By the strong Markov property $P(F_\varepsilon)$ is a product of three factors. In the second, P_1 is at distance ε from edge 1 of the translated wedge $C_{a+\varepsilon e_1}$; the kernel is smooth up to the edges away from the apex and vanishes on them (Lemma 2(a)), so the exit density is $\varepsilon\,\frac{1}{2}\partial_{n_1}\partial_{n_2}p_{t-s}(P_1,P_2)+o(\varepsilon)$, locally uniformly. In the third, P_2 is at distance ε from edge 2 of $C_{a+\varepsilon\mathbf{1}}$, and the survival probability is $\varepsilon\,\partial_{n_2}S_{1-t}(P_2)+o(\varepsilon)$. Hence $\varepsilon^{-2}P(F_\varepsilon)\to\frac{1}{4}\,\partial_{n_1}p_s\,\partial_{n_1}\partial_{n_2}p_{t-s}\,\partial_{n_2}S_{1-t}\,ds\,dt\,dr_1\,dr_2$. Step 3. By Lemma 1, on F_ε the path stays in $C_{a+\varepsilon\mathbf{1}}$ and reaches both lines, so $M_i\in[a_i,a_i+\varepsilon)$. Conversely, a path in $E_\varepsilon=\{M_i\in[a_i,a_i+\varepsilon),\ i=1,2,\ \theta_1<\theta_2\}$ that is not of type F_ε leaves C_a through edge 2 first and must later come within ε of edge 1 and again of edge 2; each such approach that the path survives costs a factor $O(\varepsilon)$ as in Step 2, so this has probability $O(\varepsilon^3)$, locally uniformly. Finally, conditionally on F_ε, θ_1 and θ_2 differ from the two exit times, and G,H from $r_1\sin\alpha, r_2\sin\alpha$, by $o(1)$ in probability (Remark 1). Step 4. So $\varepsilon^{-2}P(E_\varepsilon\cap\cdot)$ and $\varepsilon^{-2}P(F_\varepsilon\cap\cdot)$ have the same limit against continuous functions with compact support in the open domain, dominated by Lemma 4. By Lemma 1, $dr_1\,dr_2=dg\,dh/\sin^2\alpha$, and the levels a_i are distances to the edges since $|u_i|=1$. □

The three factors are the three pieces of the path: to edge 1, from edge 1 to edge 2, and survival from edge 2. Each touch carries the factor $\frac{1}{2}$ of an exit flux, hence $\frac{1}{4}$. At $\alpha=\pi/2$, after integration over the gaps, the formula factorizes into two copies of the one-motion law of [1], with density $\frac{a}{\sqrt{2\pi}\,s^{3/2}}e^{-a^2/(2s)}\sqrt{2/(\pi(1-s))}$ for (M,θ); this fixes the constant independently.

Remark 1 (The step argued at the level of densities). The last sentence of Step 3 in the proof of Theorem 1, that given F_ε the argmax times and gaps differ from the exit times and exit distances by $o(1)$ in probability, is the planar counterpart of the path decomposition at the maximum [2]: a path started ε below a level and conditioned never to cross it moves away like a meander, so its closest approach comes within a time that vanishes with ε. We use this for each coordinate but have not written out the limit for the planar path, whose coordinates are conditioned jointly; it is the one step of Theorem 1 argued at the level of densities. Its consequences are checked independently: at $\alpha=\pi/2$ the formula reduces exactly to [1], and Sections 2 and 3 compare it with the arcsine law, with [4] and with simulation.

Method. The series of Lemma 2, cut by Lemma 3, enter Corollary 1, integrated by a fixed tensor quadrature. Theorem 1 must reproduce: the classical formulas at $\rho=0$; the arcsine marginals of f_ρ; $P(\theta_1<\theta_2)=1/2$; and, from the same survival series, $c(\rho)=E[M_1M_2]$ of Rogers and Shepp [4].

Parameters. k is kept on $x,y\le X=\sqrt{2E}/\min(1,\sin\alpha)$, $E=40$, beyond which it is below e^{-40} times a polynomial (Lemma 4(ii)); Gauss–Legendre in v, $x=Xv^2$, at least 160 nodes and ten per unit length, checked at one and a half times as many. Marginals at $s=0.05,\,0.2,\,0.5,\,0.8$ for $\rho=-0.5,\,0,\,0.5,\,0.9$; the symmetry on 53 correlations; [4] at nine correlations in $[-0.9,0.9]$. Tolerances, fixed in advance: 10^{-8} relative against closed forms, 2×10^{-6} for masses, 10^{-7} against [4].

Result. At $\rho=0$ the series reproduce δ to 1.3×10^{-11} and k to 1.7×10^{-16}, and f_0 the arcsine product to a relative 5.8×10^{-12}. The marginals agree with the arcsine density to

a relative 7.7×10^{-11}; $P(\theta_1 < \theta_2)$ is within 1.1×10^{-8} of $1/2$; $E[M_1 M_2]$ agrees with [4] to 4.1×10^{-13} at all nine correlations, and the simulation of Section 3 with [4] within 1.36 standard errors at all ten of its correlations, including $\rho = 0.99$, where only simulation is used. In passing, [4] gives $c(-1/2) = 0.500000000000$ and $c(1/2) = 0.7990381057$, equal to $(3\sqrt{3} - 2)/4$ within 1.2×10^{-16}: numerical observations we do not pursue.

Error. Every comparison is inside its tolerance by two orders of magnitude or more; the largest discrepancy against a closed form is 7.7×10^{-11}. The constants of Theorem 1 are thus confirmed independently of Remark 1.

Script. `fig_wedge.py`: one simulated pair at $\rho = 0.5$ from `results.npz`, as two time series and as the planar path with the two edges of C_M.

Shows. Lemma 1 and Theorem 1.

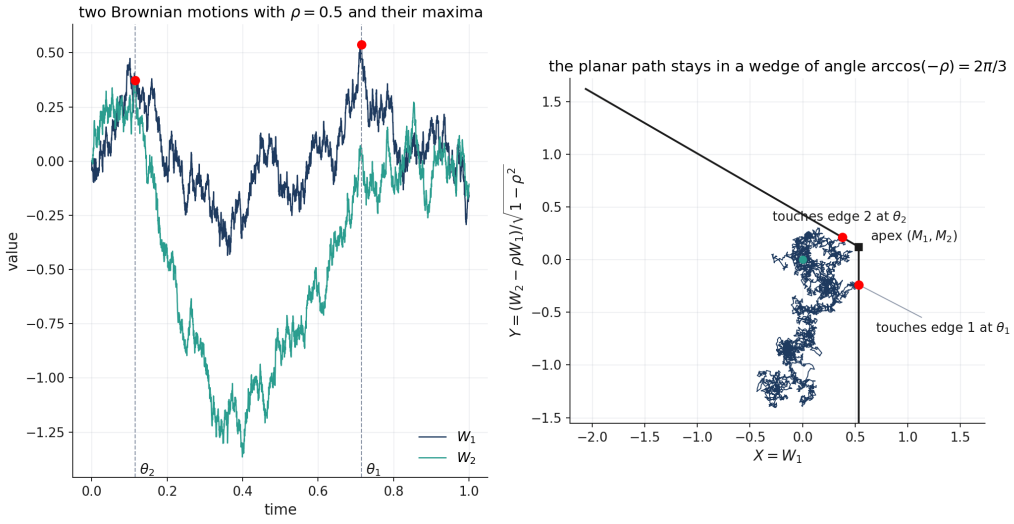


Figure 1: Left, two Brownian motions with correlation one half and the times of their maxima; right, the same pair as one planar path, which stays inside the wedge with apex at the two maxima and angle two thirds of pi and touches each edge once, at the time of the corresponding maximum.

In this sample $\theta_2 < \theta_1$, the mirror case of Theorem 1.

3. The Joint Density

Corollary 1 (The joint density of the two times)**.** For $0 < s < t < 1$, $u = t - s$, $L = 1 - t$, the density of (θ_1, θ_2) is

$$f_\rho(s,t) = \frac{\sin\alpha}{4} \iint D_s(r_1) K_u(r_1, r_2) D_L(r_2)\, dr_1 dr_2$$
$$= \frac{\sin\alpha}{4u\sqrt{sL}} \iint \delta\Big(\sqrt{\tfrac{u}{s}}\, x\Big) k(x,y)\, \delta\Big(\sqrt{\tfrac{u}{L}}\, y\Big) dx\, dy,$$

integrals over $(0,\infty)^2$; $f_\rho(s,t) = f_\rho(t,s) = f_\rho(1-t, 1-s)$, and $|\theta_1 - \theta_2|$ has the density $g_\rho(u) = 2\int_0^{1-u} f_\rho(s, s+u)\, ds$.

Proof. Integrate Theorem 1 over the gaps, $dg\,dh = \sin^2\alpha\, dr_1 dr_2$, and over the levels: the map $z \mapsto (a_1, a_2)$ to the distances from the edges is linear with Jacobian $\sin\alpha$. By the symmetry of the heat kernel and Lemma 4(i),

$$\int_C \partial_{n_1} p_s(z, P_1)\, dA(z) = \partial_{n_1} \int_C p_s(P_1, z)\, dA(z) = \partial_{n_1} S_s(P_1) = D_s(r_1);$$

the last factor is $D_L(r_2)$ by the symmetry of the wedge, the middle one $K_u(r_1, r_2)$, and the constant is $\frac{1}{4}\sin\alpha$. Lemma 2(c), (d) with $r_i = \sqrt{u}\, x_i$ give the second form. Reflection in the bisector maps D and K to themselves, so $f_\rho(s,t) = f_\rho(t,s)$; the pair $W_i(1-v) - W_i(1)$ has correlation ρ and maxima at $1-\theta_i$, so $f_\rho(s,t) = f_\rho(1-t, 1-s)$. □

The integral is finite by Lemma 4. It is a double integral of two convergent Bessel series, not a closed form; Section 6 gives the correlations at which its integrand is elementary.

Proposition 1 (The diagonal law)**.** Let (M_1', M_2') be an independent copy of (M_1, M_2). For $0 < t < 1$,

$$P(\theta_1 \le t,\ \theta_2 \le t) = P(\sqrt{t}\, M_i \ge \sqrt{1-t}\, M_i',\ i = 1, 2) = E[Q(\lambda M_1, \lambda M_2)],$$

where $\lambda = \sqrt{t/(1-t)}$ and $Q(b) = P(M_1 < b_1, M_2 < b_2)$ is the probability that the planar path stays in C_b.

Proof. As each maximum is attained once [1], $\theta_i \le t$ if and only if $X_i \ge Y_i$, with $X_i = \sup_{v \le t} W_i(v) - W_i(t)$ and $Y_i = \sup_{v \ge t} W_i(v) - W_i(t)$, up to a null set. (X_1, X_2) depends on the increments on $[0, t]$ and (Y_1, Y_2) on those on $[t, 1]$, so they are independent. Reversing time on $[0, t]$ gives again a ρ-correlated pair, so by scaling (X_1, X_2) has the law of $\sqrt{t}\,(M_1, M_2)$, and by the Markov property (Y_1, Y_2) that of $\sqrt{1-t}\,(M_1', M_2')$. Conditioning on M gives the second form, by Lemma 1. □

The identity is exact but not a closed form: it is an expectation over the law of (M_1, M_2) [5]. At $\rho = 0$ it is $(\frac{2}{\pi}\arcsin\sqrt{t})^2$; near $t = 0$ it gives the corner exponent of Proposition 2(b).

Algorithm 1 — Exact-extremum Monte Carlo for a correlated pair

Inputs: ρ; n base steps, $h = 1/n$; K candidate steps per motion; $m(\rho) = \max(32, \lceil 25/(1-\rho^2)\rceil)$ sub-steps; the number of pairs; a seed. *Output:* samples of $(\theta_1, \theta_2, M_1, M_2)$; for a bridge, the path is pinned.

1. Draw $Z = (X, Y)$ at the times kh from Gaussian increments (for a bridge subtract $kh\, Z(1)$); set $W_1 = X$, $W_2 = \rho X + \bar{\rho} Y$.
2. For each motion take the K steps with the largest endpoint value; take the union over the two motions.
3. Refine each chosen step jointly in the plane into $m(\rho)$ sub-steps by exact two-dimensional Brownian-bridge interpolation.
4. In every sub-step and every other base step, draw for each motion the exact

Brownian-bridge maximum between endpoint values x, y over the length ℓ: $\frac{1}{2}(x+y+\sqrt{(y-x)^2-2\ell\log U})$, U uniform.

5. For each motion the step with the largest maximum wins; its maximum is M_i.
6. In the winning step, with $A = M_i - x$, $B = M_i - y$: with probability $B/(A+B)$ draw V inverse Gaussian with mean A/B and shape A^2/ℓ, otherwise $V = 1/V'$ with V' inverse Gaussian with mean B/A and shape B^2/ℓ; set θ_i to the start of the step plus $\ell V/(1+V)$.
7. Repeat; rerun with $2n$ steps as a step-halving check.

Cost. $O(n + Km(\rho))$ per pair; $m(\rho)$ is 32 at $\rho = 0$ and 50, 132, 1257 at $\rho = 0.7$, 0.9, 0.99.

Steps 4 and 6 are exact for each motion: the bridge maximum [23] and the location of the maximum given its value, as in retrospective exact simulation [24]; we derived the two-branch form from the joint law of a bridge's maximum and its time. Within one sub-step the two motions are drawn independently given the endpoints, exact marginally but not jointly; the rule for $m(\rho)$ keeps the sub-step scale $\sqrt{h/m(\rho)}$ below $\sqrt{1-\rho^2}\sqrt{h}/5$, so that near-ties of the two maxima are resolved. A first run with $m = 32$ throughout failed the step-halving check of the gap law at $\rho = 0.99$; this rule was fixed before the second run.

Method. f_ρ is evaluated on an (s,u) grid whose map $u = z^{1/b}$, $b = \min(\pi/\alpha - 1, 1)$, absorbs the diagonal singularity; moments, the diagonal law ($2\iint_{s<s'\le t} f_\rho$), the joint distribution function and g_ρ follow, and doubled grids give the error. Algorithm 1 tests all of them, the arcsine marginals and $P(\theta_1 < \theta_2) = 1/2$, with a step-halving rerun.

Parameters. 96 Gauss–Legendre nodes in z, 97 tanh–sinh nodes in $s/(1-u)$; g_ρ on logarithmic grids down to $u = 10^{-12}$ and $1 - u = 10^{-9}$. Simulation at ten correlations, 1,200,000 pairs each in three seeds, $n = 1000$, $K = 12$; the diagonal law at 15 values of t, the gap law at nine values of u, the distribution function at seven points. Tolerances: $|z| \le 4$, chi-square $p \ge 10^{-4}$, 2×10^{-6} for masses.

Result. Doubling the grids changes $E[\theta_1\theta_2]$ by at most 2.1×10^{-9} over 53 correlations. At $\rho = 0$ the diagonal law agrees with $(\frac{2}{\pi}\arcsin\sqrt{t})^2$ to 2.0×10^{-11} and the distribution function with the arcsine product to 3.0×10^{-10}. The gap density integrates to 1 within 4.3×10^{-7}. Against simulation the largest $|z|$ is 3.15 for the diagonal law (Table 1), 2.30 for the gap law, 2.65 for the distribution function and 1.88 for $P(\theta_1 < \theta_2)$; the smallest chi-square p for the marginals is 0.059; halving the step moves the correlation by at most 1.49 and the gap law below $u = 0.03$ by at most 1.56 standard errors.

Error. The quadrature error, of order 10^{-9}, is far below the sampling error, and every simulated quantity is within 3.15 standard errors of the formula.

Source. Quadrature of Corollary 1 for the formula values, and Algorithm 1 with 1,200,000 pairs per correlation for the simulated column; `numbers.json`, `CHECKS.txt`, `derive.py`.

Columns. The correlation; $P(\theta_1 \le t, \theta_2 \le t)$ from the formula at five values of t; the largest $|z|$ of the simulated diagonal law against the formula over all 15 tested values of t (no simulation at $\rho = -0.99$). The row $\rho = 0$ is $(\frac{2}{\pi}\arcsin\sqrt{t})^2$.

Table 1: The probability that both maxima occur before t (Proposition 1), from the formula, with the largest deviation of simulation from it.

ρ	$t = 0.1$	$t = 0.3$	$t = 0.5$	$t = 0.7$	$t = 0.9$	**MC max $\lvert z \rvert$ (15 t)**
-0.99	0.00017	0.01871	0.10254	0.28069	0.59050	–
-0.9	0.00113	0.02984	0.11981	0.29182	0.59147	3.15
$-1/\sqrt{2}$	0.00586	0.05308	0.15151	0.31506	0.59620	0.96
-0.5	0.01385	0.07727	0.18169	0.33925	0.60418	1.78
0	0.04196	0.13617	0.25000	0.39815	0.63229	1.33
$+0.5$	0.08429	0.20493	0.32568	0.46691	0.67462	1.53
$+0.9$	0.14714	0.29357	0.42050	0.55555	0.73748	1.27
$+0.99$	0.18573	0.34443	0.47418	0.60641	0.77606	1.39

Script. `fig_heat.py`: $\log_{10} f_\rho$ on a 160×160 grid for six correlations, from `results.npz`.

Shows. Corollary 1 and Proposition 2.

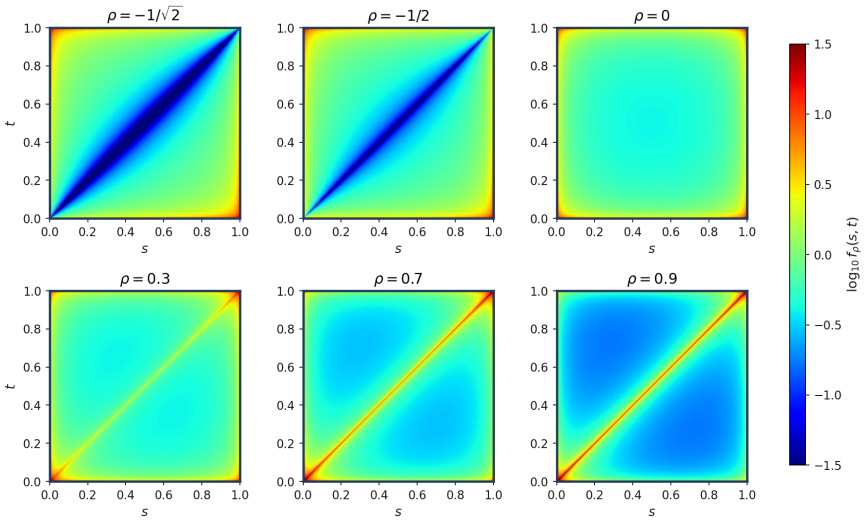


Figure 2: The joint density of the two argmax times on the unit square for six correlations from minus one over root two to nine tenths, on a logarithmic color scale; for negative correlation the density vanishes along the diagonal, at zero it is a product of arcsine laws, and for positive correlation it concentrates on the diagonal.

For $\rho < 0$ the density is largest near $(0, 1)$ and $(1, 0)$, where one maximum comes first and the other last.

Script. `fig_gap.py`: g_ρ for five correlations with simulated histograms, from `results.npz` and `numbers.json`.

Shows. The gap law of Corollary 1 and Proposition 2(c).

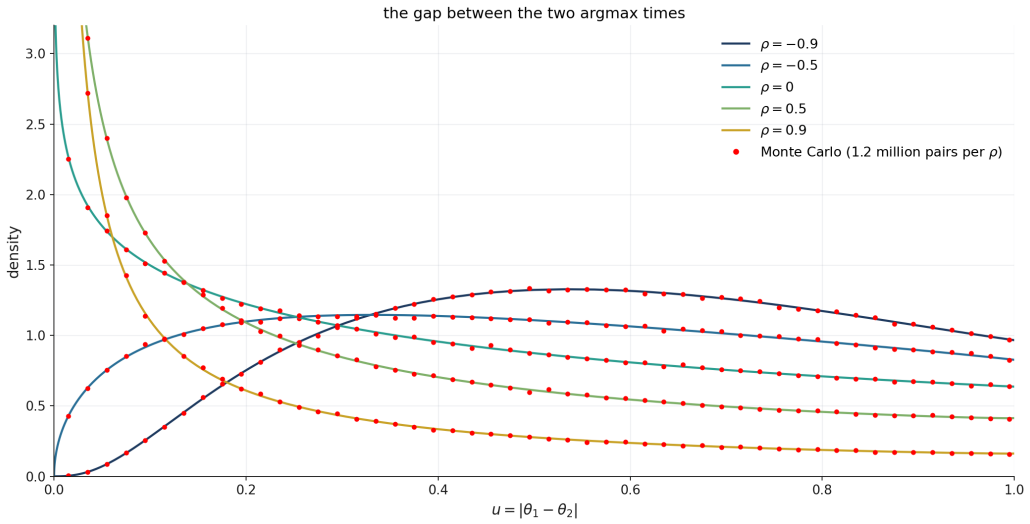


Figure 3: The density of the distance between the two argmax times for correlations minus nine tenths, minus one half, zero, one half and nine tenths, with simulated histograms as dots; it vanishes at zero for negative correlation, diverges slowly for zero correlation, and diverges like a power for positive correlation.

At $\rho = -0.9$ the density is flat at 0, where it vanishes like $u^{2.4827}$ (Table 2).

4. Local Behavior and a Coincidence Dichotomy

Proposition 2 (Local exponents)**.** Let $p = \pi/\alpha$, c_α as in Lemma 2(e), and

$$I_\alpha = \iint x^{p-1} k(x,y)\, y^{p-1}\, dx\, dy, \qquad \Psi(s,t) = \frac{\sin\alpha}{4}\, c_\alpha \iint D_s(r_1)\, K_{t-s}(r_1,r_2)\, r_2^{p-1}\, dr_1\, dr_2,$$

integrals over $(0,\infty)^2$, both finite. Then: (a) for fixed $s \in (0,1)$, $f_\rho(s, s+u) = \frac{\sin\alpha}{4} c_\alpha^2 I_\alpha [s(1-s)]^{-p/2} u^{p-2}(1+o(1))$ as $u \downarrow 0$; (b) for fixed $0 < s < t$, $f_\rho(\varepsilon s, \varepsilon t) = \varepsilon^{p/2-2}\Psi(s,t)(1+o(1))$ as $\varepsilon \downarrow 0$, and $P(\theta_1 \le \varepsilon, \theta_2 \le \varepsilon) \sim C_{\mathrm{c}}\, \varepsilon^{p/2}$ with $C_{\mathrm{c}} = (c_\alpha/p)\, E[R^p \sin(p\beta)] \in (0,\infty)$, where (R,β) are the polar coordinates of the point at distances M_1, M_2 from the two edges; (c) as $u \downarrow 0$: for $\rho > 0$, $g_\rho(u) \sim \frac{\sin\alpha}{2} c_\alpha^2 I_\alpha B(1-\frac{p}{2}, 1-\frac{p}{2})\, u^{p-2}$; for $\rho = 0$, $g_0(u) = \frac{4}{\pi^2}\log(1/u) + O(1)$; for $\rho < 0$, $g_\rho(u) \sim 4\int_0^\infty \Psi(\sigma, \sigma+1)\, d\sigma\; u^{p/2-1}$, the mass coming from the corners $(0,0)$ and $(1,1)$.

Proof. By Lemma 4(ii), (iii), $\delta(x) \le Cx^{p-1}$, $k(x,y) \le C(xy)^{p-1}$ and k has a Gaussian bound, so $I_\alpha < \infty$; with $D_s \le \sqrt{2/(\pi s)}$, Ψ is finite too. (a) With $\varepsilon_1 = \sqrt{u/s}$, $\varepsilon_2 = \sqrt{u/L}$, $L = 1-s-u$, the scaled form of Corollary 1 reads $u^{2-p} f_\rho(s, s+u) = \frac{\sin\alpha}{4}(sL)^{-p/2} \iint \varepsilon_1^{1-p}\delta(\varepsilon_1 x)\, k(x,y)\, \varepsilon_2^{1-p}\delta(\varepsilon_2 y)\, dx\, dy$. The integrand tends to $c_\alpha^2 x^{p-1}k(x,y)y^{p-1}$ by Lemma 2(e) and is dominated by $C^2 x^{p-1}k(x,y)y^{p-1}$. (b) Put $r_i = \sqrt{\varepsilon}\,\varrho_i$ in Corollary 1 at $(\varepsilon s, \varepsilon t)$. By Lemma 2(c), (d), $D_{\varepsilon s}(\sqrt{\varepsilon}\varrho_1) = \varepsilon^{-1/2} D_s(\varrho_1)$ and $K_{\varepsilon u}(\sqrt{\varepsilon}\varrho_1, \sqrt{\varepsilon}\varrho_2) = \varepsilon^{-2} K_u(\varrho_1,\varrho_2)$, while $\varepsilon^{-(p-1)/2} D_{1-\varepsilon t}(\sqrt{\varepsilon}\varrho_2) \to c_\alpha \varrho_2^{p-1}$ (Lemma 2(e)) and is at most $C\varrho_2^{p-1}$ (Lemma 4(iii)). The powers add to $-\frac{1}{2} - 2 + 1 + \frac{p-1}{2} = \frac{p}{2} - 2$; dominated convergence gives the density. For the probability, Proposition 1 gives $E[Q(\lambda M)]$ with $\lambda = \sqrt{\varepsilon/(1-\varepsilon)}$; the

point at distances $\lambda M_1, \lambda M_2$ has polar coordinates $(\lambda R, \beta)$, so $\lambda^{-p} Q(\lambda M) \to (c_\alpha/p) R^p \sin(p\beta)$ by Lemma 2(e) and $\lambda^{-p} Q(\lambda M) \le C R^p$ by Lemma 4(iii), which is integrable. $C_c > 0$ as $\sin(p\beta) > 0$ on $(0, \alpha)$. (c) The bounds in (a) give, for all s, u, $f_\rho(s, s+u) \le C u^{p-2} (sL)^{-p/2}$ (call it (B)). Write $g_\rho(u) = 2(1-u) \int_0^1 f_\rho(s_\sigma, s_\sigma + u)\, d\sigma$ with $s_\sigma = (1-u)\sigma$, so $s_\sigma L = (1-u)^2 \sigma(1-\sigma)$. If $\rho > 0$, then $p < 2$, $[\sigma(1-\sigma)]^{-p/2}$ is integrable, and (B), (a) and dominated convergence give the Beta integral. If $\rho = 0$, $f_0(s,t) = \pi^{-2} [s(1-s)t(1-t)]^{-1/2}$; by $s \mapsto 1-u-s$ the two halves of $[0, 1-u]$ contribute equally, on the first half $[(1-s)(1-s-u)]^{-1/2} = 1 + O(s+u)$, and $\int_0^{(1-u)/2} ds/\sqrt{s(s+u)} = 2 \operatorname{arsinh} \sqrt{(1-u)/(2u)} = \log(1/u) + O(1)$, so $g_0(u) = 2 \cdot 2\pi^{-2} \log(1/u) + O(1)$. If $\rho < 0$, then $p > 2$. Fix $A > 1$ and split $[0, 1-u]$ into $[0, Au]$, a middle part and $[1-u-Au, 1-u]$, the last equal to the first by $f_\rho(s,t) = f_\rho(1-t, 1-s)$. By (B), the middle contributes at most $C u^{p-2} \int_{Au}^\infty s^{-p/2} ds = C' A^{1-p/2} u^{p/2-1}$. On the first part, $s = u\sigma$ turns the contribution into $2u^{p/2-1} \int_0^A u^{2-p/2} f_\rho(u\sigma, u(\sigma+1))\, d\sigma$, and by (b), with the domination from its proof, into $2u^{p/2-1} \int_0^A \Psi(\sigma, \sigma+1)\, d\sigma\, (1 + o(1))$. Since $D_\sigma(\varrho) \le C \sigma^{-p/2} \varrho^{p-1}$, $\Psi(\sigma, \sigma+1) \le C \sigma^{-p/2} I_\alpha$ is integrable at infinity, and letting $A \to \infty$ gives the claim. □

The diagonal exponent $p - 2$ comes from two factors $\delta \approx c_\alpha x^{p-1}$ at the ends of a short passage between the edges, the corner exponent from one; $p/2 = \pi/(2\alpha)$ is the survival exponent of the wedge [8], [9], which also governs walks in cones [17].

Corollary 2 (Repulsion, neutrality and attraction)**.** For $s \in (0,1)$, as $u \downarrow 0$, $f_\rho(s, s+u)$ tends to 0 if $\rho < 0$, to $1/(\pi^2 s(1-s))$ if $\rho = 0$ and to $+\infty$ if $\rho > 0$: the joint density blows up on the open diagonal if and only if $\rho > 0$. The density g_ρ of $|\theta_1 - \theta_2|$ vanishes at 0 if and only if $\rho < 0$, diverges logarithmically at $\rho = 0$ and like a power for $\rho > 0$, and $P(|\theta_1 - \theta_2| \le u)$ is of exact order $u^{\pi/(2\alpha)}$, $u \log(1/u)$ and $u^{\pi/\alpha - 1}$ in the three cases.

Proof. The exponent $\pi/\alpha - 2$ of Proposition 2(a) is positive, zero or negative as $\alpha < \pi/2$, $= \pi/2$ or $> \pi/2$, that is as $\rho < 0$, $= 0$ or > 0; at $\rho = 0$ the density is the arcsine product. The rest is Proposition 2(c), integrated from 0 to u. □

For $\rho < 0$ the maxima avoid each other inside $[0,1]$ and nearly coincide only when both occur at the very start or both at the very end. This is the argmax counterpart of the dichotomy of Kou and Zhong [11] for first-passage times through the same wedge, where the density of the difference of the passage times blows up at 0 if and only if $\rho > 0$; here the exponents are explicit. The same sign condition separates the regimes of the reflected motion in a wedge [16].

Method. Local slopes of the formula at the smallest scales: $\log f_\rho(\varepsilon, 2\varepsilon)$ against $\log \varepsilon$ (corner), $\log f_\rho(0.4, 0.4+u)$ against $\log u$ (diagonal), $\log g_\rho$ (gap), and $\log \kappa$ at $u = 10^{-5}$ (bridge, Theorem 6), against Proposition 2. The constants: the ratio of $f_\rho(0.4, 0.4+u)$ to the leading term of Proposition 2(a); $u^{2-p} g_\rho(u)$ against Proposition 2(c); the coefficient of $\log(1/u)$ in g_0. Simulation: slopes of the corner mass $P(\theta_1 \le \varepsilon, \theta_2 \le \varepsilon)$ and gap mass $P(|\theta_1 - \theta_2| \le u)$ over a window holding at least 2000 events at its lower end, against the formula's slope on the same window, since the asymptotic regime lies at smaller scales.

Parameters. The eleven correlations of Table 2, scales down to 10^{-9} for f_ρ and 10^{-12} for g_ρ; the constants at $\rho = -0.5,\ 0.3,\ 0.5,\ 0.7,\ 0.9,\ 0.99$; simulation as in Section 3. Tolerances, fixed in advance: 0.02 for an analytic slope, 0.1 for a simulated slope against the formula.

Result. Table 2: corner slopes within 4.6×10^{-6} of $p/2-2$, diagonal slopes within 9.2×10^{-6} of $p-2$, gap slopes within 0.0100 and bridge slopes within 0.0264 of their predictions, the largest deviations at $\rho=-0.99$, where the diagonal exponent is 20.1959. At $\rho=0$ the gap slope is -0.0345 and the coefficient of $\log(1/u)$ between $u=10^{-12}$ and 10^{-6} is 0.405283 against $4/\pi^2 = 0.405285$. The diagonal ratio is within 6.1×10^{-9} of 1 at $u=10^{-9}$ for all six correlations. The gap constant at $u=10^{-12}$ against the formula: $\rho=0.3$: 1.60343 against 1.61720; $\rho=0.5$: 0.78348 against 0.78395; $\rho=0.7$: 0.41629 against 0.41631; $\rho=0.9$: 0.17658 against 0.17658; $\rho=0.99$: 0.04738 against 0.04738. In simulation, both window slopes at every simulated correlation agree with the formula within 0.007.

Error. The exponents are confirmed to the accuracy of a finite-difference slope. The gap constant is within a relative 6.1×10^{-4} for $\rho\ge0.5$ and 0.0085 at $\rho=0.3$, where $p=1.6751$ and the corner term of the proof, smaller by a factor of order $u^{1-p/2}$, is still 0.011 at $u=10^{-12}$.

Source. Local slopes of the formula of Corollary 1 at the smallest scales (ε, u down to 10^{-9} for the density, 10^{-12} for the gap density), and of the bridge density κ of Theorem 6 at $u=10^{-5}$; `numbers.json`, `results.npz`, `derive.py`.

Columns. The correlation; the local slope of $f_\rho(\varepsilon,2\varepsilon)$ in ε and its prediction $p/2-2$ (Proposition 2(b)); the local slope of $f_\rho(0.4,0.4+u)$ in u and its prediction $p-2$ (Proposition 2(a)); the local slope of the gap density and its prediction, $p/2-1$ for $\rho<0$ and $p-2$ for $\rho>0$ (Proposition 2(c)); the local slope of κ, whose prediction is $p-2$ (Theorem 6).

Table 2: Local exponents of the joint density, the gap density and the bridge gap density, measured on the formula, against Proposition 2 and Theorem 6.

ρ	**corner slope**	$\pi/(2\alpha)-2$	**diagonal slope**	$\pi/\alpha-2$	**gap slope**	**predicted**	**bridge slope**
-0.99	9.0979	9.0979	20.1959	20.1959	10.1079	10.0979	20.1695
-0.9	1.4827	1.4827	4.9654	4.9654	2.4837	2.4827	4.9646
$-\sqrt{3}/2$	1.0000	1.0000	4.0000	4.0000	2.0014	2.0000	3.9995
$-1/\sqrt{2}$	0.0000	0.0000	2.0000	2.0000	1.0003	1.0000	1.9999
-0.5	-0.5000	-0.5000	1.0000	1.0000	0.5000	0.5000	1.0000
0	-1.0000	-1.0000	0.0000	0.0000	-0.0345	0 (log)	0.0000
$+0.3$	-1.1625	-1.1625	-0.3249	-0.3249	-0.3263	-0.3249	-0.3249
$+0.5$	-1.2500	-1.2500	-0.5000	-0.5000	-0.5002	-0.5000	-0.5000
$+0.7$	-1.3305	-1.3305	-0.6610	-0.6610	-0.6610	-0.6610	-0.6610
$+0.9$	-1.4162	-1.4162	-0.8324	-0.8324	-0.8324	-0.8324	-0.8324
$+0.99$	-1.4764	-1.4764	-0.9528	-0.9528	-0.9528	-0.9528	-0.9528

5. The Correlation of the Times

Theorem 2 (The chaos structure of the correlation)**.** Let $\theta = \operatorname{argmax}_{[0,1]} W$ for a standard Brownian motion W, $F = \theta - \frac{1}{2}$, and $J_n F$ the projection of F on the n-th Wiener chaos of W. For every $\rho \in [-1,1]$,

$$\operatorname{corr}(\theta_1,\theta_2) = \sum_{n\geq 1} c_n \rho^n,$$
$$c_n = 8\|J_n F\|^2 \geq 0,$$
$$\sum_{n\geq 1} c_n = 1,$$
$$\sum_{n\geq 1} (-1)^n c_n = \frac{6-7\zeta(3)}{4} = -0.6035996.$$

Hence $\sum_{n \text{ odd}} c_n = (7\zeta(3)-2)/8 = 0.801800$, $\sum_{n \text{ even}} c_n = (10-7\zeta(3))/8 = 0.198200$, and the correlation is continuous on $[-1,1]$, real-analytic on $(-1,1)$, and increasing and convex on $[0,1]$.

Proof. F is bounded, and by the arcsine law $EF = 0$ and $\operatorname{Var}\theta = \frac{1}{8}$, so $F = \sum_{n\geq 1} J_n F$ in L^2 [19]. For $\rho \in [0,1]$ couple $W_2 = \rho W_1 + \bar{\rho} W'$ with W' an independent Brownian motion. By Mehler's formula, $E[G(\rho W_1 + \bar{\rho} W') \mid W_1] = T_\rho G(W_1)$, where the Ornstein–Uhlenbeck operator T_ρ at time $-\log\rho$ multiplies the n-th chaos by ρ^n [19]; so

$$\operatorname{cov}(\theta_1,\theta_2) = E[F\,T_\rho F] = \sum_n \rho^n \|J_n F\|^2.$$

For $\rho < 0$ write $\rho W_1 + \bar{\rho} W' = |\rho|(-W_1) + \bar{\rho} W'$; the map $w \mapsto -w$ multiplies the n-th

chaos by $(-1)^n$. *Divide by* $\operatorname{Var}\theta = \frac{1}{8}$. *At* $\rho = 1$ *the correlation is* 1*; at* $\rho = -1$, θ_2 *is the time of the minimum of* W_1 *and* $\operatorname{cov}(t_{\max}, t_{\min}) = -(7\zeta(3) - 6)/32$ *[13]. The odd and even sums are half the sum and half the difference of the two values. A power series with non-negative coefficients of finite sum converges uniformly on* $[-1, 1]$, *and on* $[0, 1]$ *each term is increasing and convex.* □

Nothing here is special to the argmax beyond the two endpoint values. The correlation itself has no closed form: only the two sums and c_1 (Theorem 3) are exact.

Theorem 3 (The slope at independence)**.** For $\theta = \operatorname{argmax}_{[0,1]} W$,

$$h(u) = \frac{d}{du}E[\theta W(u)] = \sqrt{\tfrac{2}{\pi}}\,(\sqrt{u} + \sqrt{1-u} - 1),$$
$$E[\theta W(u)] = \sqrt{\tfrac{2}{\pi}}\Big[\tfrac{2}{3}u^{3/2} + \tfrac{2}{3}(1 - (1-u)^{3/2}) - u\Big],$$

and $c_1 = 8\int_0^1 h^2 = 4 - 32/(3\pi) = 0.604694547$, so

$$\operatorname{corr}(\theta_1, \theta_2) = (4 - \frac{32}{3\pi})\rho + O(\rho^2).$$

Proof. $J_1 F = \int_0^1 h\,dW$ *with* $\int_0^u h = E[\theta W(u)]$, *so* $\|J_1 F\|^2 = \int_0^1 h^2$. *Given* $\theta = s$, $(M - W(s-v))_{v \le s}$ *and* $(M - W(s+v))_{v \le 1-s}$ *are independent Brownian meanders of lengths* s *and* $1-s$ *[2]. A meander on* $[0,1]$ *has mean* $\mu(v) = \sqrt{2/\pi}[\sqrt{v(1-v)} + \arcsin\sqrt{v}]$, *from its marginal density* $(x/v^{3/2})e^{-x^2/(2v)}\operatorname{erf}(x/\sqrt{2(1-v)})$ *[23]; a meander of length* ℓ *has mean* $\sqrt{\ell}\,\mu(v/\ell)$, *and* M *is the end value of the first one. With* f *the arcsine density,*

$$E[\theta W(u)] = \mu(1)\int_0^1 s^{3/2} f(s)\,ds - \int_u^1 s^{3/2} f(s)\,\mu(1 - \tfrac{u}{s})ds - \int_0^u s\sqrt{1-s}\,f(s)\,\mu\Big(\frac{u-s}{1-s}\Big)ds.$$

Differentiate; boundary terms vanish as $\mu(0) = 0$. *With* $\mu'(v) = \sqrt{2/\pi}\sqrt{(1-v)/v}$, *the second term gives*

$$\sqrt{2/\pi}\frac{\sqrt{u}}{\pi}\int_u^1 \frac{ds}{\sqrt{(s-u)(1-s)}} = \sqrt{2/\pi}\sqrt{u}$$

and the third

$$-\sqrt{2/\pi}\frac{\sqrt{1-u}}{\pi}\int_0^u \frac{\sqrt{s}\,ds}{(1-s)\sqrt{u-s}} = -\sqrt{2/\pi}(1 - \sqrt{1-u}),$$

the last integral being $\pi(1/\sqrt{1-u} - 1)$ *by* $s = u\sin^2\phi$. *Then*

$$\int_0^1 h^2 = \frac{2}{\pi}(2 + \frac{\pi}{4} - \frac{8}{3}) = \frac{2}{\pi}(\frac{\pi}{4} - \frac{2}{3}),$$

using $\int_0^1 \sqrt{u(1-u)}\,du = \pi/8$, *and* $c_1 = 8\int_0^1 h^2$ *by Theorem 2.* □

h is positive inside $(0,1)$, since $\sqrt{u} + \sqrt{1-u} \ge 1$: an upward increment moves the maximum later on average. The remaining share $1 - c_1$ of the variance sits in higher chaoses, known only numerically (Remark 2).

Corollary 3 (Two-sided bounds)**.** Let $c_1 = 4 - 32/(3\pi)$, $S_{\text{odd}} = (7\zeta(3) - 2)/8$, $S_{\text{even}} = (10 - 7\zeta(3))/8$. For $\rho \in [0, 1]$, $c_1\rho \le \operatorname{corr}(\theta_1, \theta_2) \le c_1\rho + (1 - c_1)\rho^2$; for $\rho = -r \in [-1, 0]$, $-c_1 r - (S_{\text{odd}} - c_1)r^3 \le \operatorname{corr}(\theta_1, \theta_2) \le -c_1 r + S_{\text{even}} r^2$. In particular $|\operatorname{corr}(\theta_1, \theta_2)| \le |\rho|$, and $\le S_{\text{odd}}|\rho| = 0.8018\,|\rho|$ for $\rho < 0$.

Proof. By Theorem 2, for $\rho \ge 0$ the terms $n \ge 2$ lie in $[0, (1 - c_1)\rho^2]$. For $\rho = -r$ the even part lies in $[0, S_{\text{even}} r^2]$ and the odd part in $[c_1 r, c_1 r + (S_{\text{odd}} - c_1)r^3]$, since $r^n \le r^3$ for odd $n \ge 3$ and $r^n \le r^2$ for even n. The upper bound is negative as $r \le 1 < c_1/S_{\text{even}}$, so $|\operatorname{corr}| \le c_1 r + (S_{\text{odd}} - c_1)r^3 \le S_{\text{odd}} r$. □

$|\operatorname{corr}| \le |\rho|$ is Gebelein's inequality [18]; the chaos structure sharpens it on both sides.

Remark 2 (Numerical observations). Read off the computed curve on 53 correlations; not proved. (a) Finite differences at 0 give $c_2 \approx 0.0564$, $c_3 \approx 0.0658$. (b) Near $\rho = 1$, $1 - \operatorname{corr}(\theta_1, \theta_2) = k_1\sqrt{1 - \rho} + k_2(1 - \rho)$ fits with $k_1 = 0.8992$, $k_2 = 0.0339$ and a free intercept of 5.0×10^{-5}, consistent with $\sum_n c_n = 1$. As $1 - \operatorname{corr} = 4E[(\theta_1 - \theta_2)^2]$, the mean square gap vanishes like $\sqrt{1 - \rho}$, linearly in $\pi - \alpha$; a Tauberian heuristic then suggests $c_n \sim \frac{k_1}{2\sqrt{\pi}} n^{-3/2} = 0.2537\, n^{-3/2}$. (c) Quadratic extrapolation from $\rho = -0.99, -0.98, -0.97$ gives -0.6035982 against the exact -0.6035996. (d) At all 52 nonzero correlations of the grid, $|\operatorname{corr}(\theta_1, \theta_2)| < |\operatorname{corr}(M_1, M_2)|$, the latter from [4]: the times are less correlated than the values.

Method. $\operatorname{corr}(\theta_1, \theta_2) = 8E[\theta_1\theta_2] - 2$ from the quadrature of Corollary 1. Theorem 3: the Richardson slope of the curve at $\rho = 0$ and the simulated $E[\theta W(u)]$. Theorem 2: the endpoint $\rho = -1$, by extrapolation. Corollary 3: its bounds, Gebelein's inequality, monotonicity and convexity on the whole curve. Simulation by Algorithm 1 at ten correlations.

Parameters. 53 correlations from -0.99 to 0.999; simulation as in Section 3; $E[\theta W(u)]$ at $u = 0.1, 0.25, 0.5, 0.75, 0.9, 1$ over all 12 million simulated paths. Tolerances: 10^{-4} for the slope, $|z| \le 4$.

Result. The slope at 0 is 0.604694546 against $c_1 = 0.604694547$, an error of 1.1×10^{-9}. Gebelein's inequality holds at all 53 correlations up to 3.1×10^{-12}, the quadrature error at $\rho = 0$, and the bounds of Corollary 3 hold at all 53; on $[0, 1)$ the smallest slope is 0.6053 and the smallest increment of the slope 1.17×10^{-3}. Extrapolation to $\rho = -1$ gives -0.6035982 against $(6 - 7\zeta(3))/4 = -0.6035996$, a difference of 1.4×10^{-6}. In simulation (Table 4) the pooled correlation agrees within 1.82 standard errors at all ten correlations and the 30 single-seed estimates within 1.95; $E[\theta W(u)]$ agrees with Theorem 3 within 3.03 at all six values of u.

Error. The slope matches c_1 to the quadrature error, the endpoint to the error of a three-point extrapolation, and the simulation stays within 3.03 standard errors.

Source. Quadrature of Corollary 1 at the correlations shown (the full curve has 53), the bounds of Corollary 3, and the formula of [4] for $\operatorname{corr}(M_1, M_2)$, interpolated from its tabulated curve; `numbers.json`, `results.npz`, `derive.py`.

Columns. The correlation; the correlation of the times; the lower and upper bounds of Corollary 3; the correlation of the two maxima.

Table 3: The correlation of the times of the maxima, with the bounds of Corollary 3, against the correlation of the values of the maxima.

ρ	$\mathrm{corr}(\theta_1, \theta_2)$	**lower bound**	**upper bound**	$\mathrm{corr}(M_1, M_2)$
-0.99	-0.5969498	-0.7899	-0.4044	-0.6832
-0.9	-0.5384334	-0.6879	-0.3837	-0.6313
$-1/\sqrt{2}$	-0.4187782	-0.4973	-0.3285	-0.5131
-0.5	-0.2952934	-0.3270	-0.2528	-0.3760
-0.1	-0.0599688	-0.0607	-0.0585	-0.0805
$+0.1$	0.0611018	0.0605	0.0644	0.0832
$+0.5$	0.3276966	0.3023	0.4012	0.4470
$+0.9$	0.7113661	0.5442	0.8644	0.8749
$+0.99$	0.9097512	0.5986	0.9861	0.9866
$+0.999$	0.9715136	0.6041	0.9986	0.9986

Source. Algorithm 1, 1,200,000 pairs per correlation in three seeds, $n = 1000$ base steps, and the rerun with $n = 2000$; the formula of Corollary 1 and the integral of [4]; `numbers.json`, `derive.py`.

Columns. The correlation; the simulated correlation of the times with its standard error from 30 batches; the formula; the z-score; the simulated correlation with twice as many steps; the simulated $E[M_1 M_2]$; its value from [4].

Table 4: Simulation against the formula for the correlation of the times, and against Rogers and Shepp for the product of the maxima.

ρ	**corr, Monte Carlo**	**corr, formula**	z	$n = 2000$	$E[M_1 M_2]$**, Monte Carlo**	**Rogers and Shepp**
-0.9	-0.53877 ± 0.00057	-0.53843	-0.60	-0.53850	0.40707	0.40722
$-\sqrt{3}/2$	-0.51752 ± 0.00053	-0.51687	-1.24	-0.51741	0.41485	0.41453
$-1/\sqrt{2}$	-0.41865 ± 0.00061	-0.41878	+0.21	-0.41895	0.44994	0.45016
-0.5	-0.29604 ± 0.00080	-0.29529	-0.93	-0.29582	0.49936	0.50000
0	-0.00160 ± 0.00097	0	-1.65	0.00056	0.63664	0.63662
$+0.3$	0.19020 ± 0.00107	0.18856	+1.53	0.19052	0.73171	0.73059
$+0.5$	0.32748 ± 0.00088	0.32770	-0.25	0.32874	0.79991	0.79904
$+0.7$	0.48942 ± 0.00067	0.48950	-0.12	0.48809	0.87322	0.87308
$+0.9$	0.71251 ± 0.00063	0.71137	+1.82	0.71189	0.95514	0.95455
$+0.99$	0.90971 ± 0.00034	0.90975	-0.11	0.91042	0.99485	0.99515

Script. `fig_corr.py`: the 53-point curve, the endpoints, the curve of [4], the slope c_1,

Gebelein's bound and simulated points, from `results.npz` and `numbers.json`.

Shows. Theorems 2 and 3, Corollary 3 and Remark 2(d).

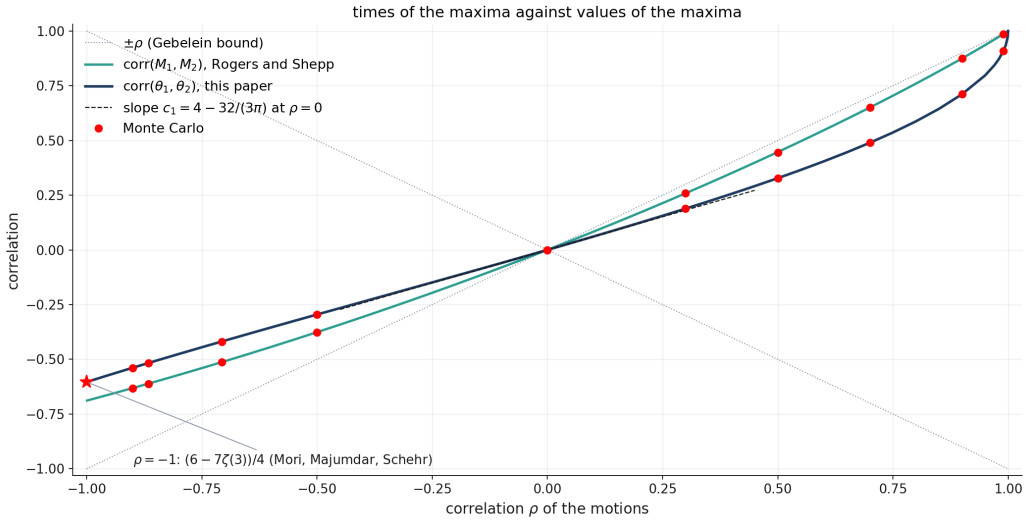


Figure 4: The correlation of the times of the maxima against the correlation of the motions, with the correlation of the maximum values of Rogers and Shepp, the exact slope four minus thirty-two over three pi at zero, the endpoint of Mori, Majumdar and Schehr at minus one, Gebelein's bound and simulated points.

The curve of the times lies inside that of the values and bends up steeply near $\rho = 1$ (Remark 2(b)).

6. Closed Forms for Dihedral Wedges

Theorem 4 (Image formulas for dihedral wedges)**.** Let $\alpha = \pi/n$, $n \geq 2$ (that is $\rho = -\cos(\pi/n)$), $\mathcal{D}_n$ the dihedral group of order $2n$ generated by the reflections in the two edges of a wedge with apex at the origin, $\operatorname{sgn} g = \det g$, $e_0 = (1,0)$, $e_\alpha = (\cos\alpha, \sin\alpha)$, $n_1 = (0,1)$, $n_2 = (\sin\alpha, -\cos\alpha)$ and Φ the standard normal distribution function. Then (i)

$$p_t(z,z') = \sum_{g\in\mathcal{D}_n} \operatorname{sgn}(g)\, g_t(z - gz'),$$

with g_t as in Lemma 4; (ii)

$$\delta(x) = \sqrt{2/\pi} \sum_{j=0}^{2n-1} (-1)^j \cos(j\pi/n)\, e^{-\frac{1}{2}x^2 \sin^2(j\pi/n)}\, \Phi(x\cos(j\pi/n));$$

(iii)

$$k(x,y) = \frac{1}{2\pi} \sum_{g} \operatorname{sgn}(g)\, [n_2 \cdot gn_1 - (w\cdot n_2)(w\cdot gn_1)]\, e^{-|w|^2/2},$$

$w = ye_\alpha - xge_0$. So f_ρ is a double integral of an elementary integrand, and $p = n$: the diagonal exponent is $n-2$ and the corner exponent $n/2-2$.

Proof. *The wedge C is a fundamental domain of $\mathcal{D}_n$: its $2n$ images tile the plane. The right-hand side $q_t(z,z')$, $z' \in C$, solves the heat equation; for z on an edge with reflection s, $sz = z$ gives $|z-sgz'| = |z-gz'|$ with opposite signs, so $q_t = 0$ there; as $t \to 0$ only $g = 1$ contributes in C; and $|q_t| \le 2n\, g_t$. By uniqueness of the Dirichlet heat kernel, $q_t = p_t$; this is the reflection argument of [20]. (ii) By (i), $S_1(z) = \sum_g \operatorname{sgn}(g) P(z+N \in gC)$, N standard Gaussian, and by the divergence theorem the gradient of $z \mapsto P(z+N \in A)$ is the flux $\oint_{\partial A} g_1(w-z)\, \nu_A(w)\, dw$ with inward normal ν_A. The chambers are bounded by the rays ℓe_j, e_j at angle $j\pi/n$, $0 \le j < 2n$; ray j separates chambers of opposite sign and opposite inward normals, so it counts twice, with sign $(-1)^j$ and normal ν_j at angle $j\pi/n + \pi/2$, and $\nu_j \cdot n_1 = \cos(j\pi/n)$. At $z = xe_0$,*

$$\int_0^\infty g_1(\ell e_j - xe_0)\, d\ell = (2\pi)^{-1/2} e^{-\frac{1}{2}x^2 \sin^2(j\pi/n)}\, \Phi(x\cos(j\pi/n)),$$

since $|\ell e_j - xe_0|^2 = (\ell - x\cos(j\pi/n))^2 + x^2 \sin^2(j\pi/n)$. (iii) Reindexing (i) by $g \mapsto g^{-1}$ gives $p_1(z,z') = \sum_g \operatorname{sgn}(g)\, g_1(z' - gz)$. With $v = z' - gz$, the derivative along n_2 in z' is $-(v \cdot n_2) g_1(v)$, and its derivative along n_1 in z, where v moves by $-gn_1$, is $[n_2 \cdot gn_1 - (v \cdot n_2)(v \cdot gn_1)] g_1(v)$; at $z = xe_0$, $z' = ye_\alpha$, $v = w$. □

At $n = 2$, (ii) is $\sqrt{2/\pi}[\Phi(x) - \Phi(-x)]$ and (iii) is $(2/\pi) xy e^{-(x^2+y^2)/2}$, as in Lemma 2(f). For larger n the terms of (ii) cancel to order x^{n-1} near 0, which the evaluation must respect.

Remark 3 (An elementary density is not yet reduced). At $\alpha = \pi/n$, $f_\rho(s,t)$ is a centered Gaussian integral in six dimensions over a polyhedral cone with four linear weights from the normal derivatives; each weight lowers the dimension by one, which suggests arctangents and square roots, as for the bridges of Proposition 3. We have not carried this out and state no closed form for f_ρ at any $\rho \neq 0$.

Method. At $n = 2$, 3, 4, 6 the image formulas of Theorem 4 are compared with the eigenseries of Lemma 2: the kernels on the quadrature grid, f_ρ at seven points, the correlation, and the diagonal law against simulation. Near $x = 0$ sum (ii) cancels to order x^{n-1} and is evaluated in extended precision.

Parameters. $\rho = 0$, $-1/2$, $-1/\sqrt{2}$, $-\sqrt{3}/2$; the grid of Section 2; 15 values of t and 1,200,000 simulated pairs. Tolerances: 10^{-10} for kernels, 10^{-8} relative for densities, 2×10^{-6} for the correlation, $|z| \le 4$.

Result. The kernels agree to 1.9×10^{-14} (δ) and 6.2×10^{-16} (k), the densities to a relative 1.5×10^{-12}. The image correlations are -0.2952934, -0.4187782, -0.5168705 at $n = 3$, 4, 6, against -0.2952934, -0.4187782, -0.5168705 from the series, within 6.4×10^{-9}. The image diagonal law agrees with simulation within 1.78 standard errors (Figure 5).

Error. Two independent evaluations, by Bessel series and by finite image sums, agree to the quadrature accuracy, the largest discrepancy being 6.4×10^{-9}, and both agree with simulation.

Script. `fig_images.py`: the diagonal law and the gap density from Theorem 4 at $\alpha = \pi/3$, $\pi/4$, $\pi/6$, with the series and simulation, from `results.npz`.

Shows. Theorem 4.

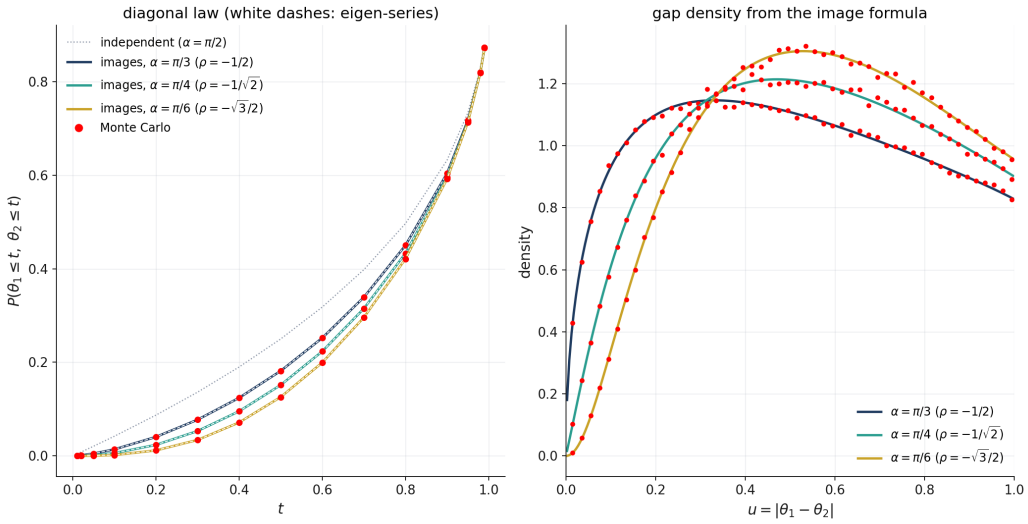


Figure 5: Left, the probability that both maxima occur before t for the wedge angles pi over three, pi over four and pi over six, from the image formulas, with the eigen-series as white dashes and simulated points; right, the gap density from the image formulas with simulated histograms.

The gap density vanishes at 0 like $u^{n/2-1}$.

7. Correlated Bridges

Definition 3 (Correlated bridges and the cyclic gap)**.** Let B_1, B_2 be standard Brownian bridges on $[0,1]$ with $E[B_1(u)B_2(v)] = \rho(\min(u,v) - uv)$, for instance $B_i(v) = W_i(v) - vW_i(1)$, with maxima at θ_1, θ_2, and let $D = (\theta_2 - \theta_1) \bmod 1 \in [0,1)$ be the cyclic gap.

Each bridge attains its maximum once, at a uniform time [21]. In the planar picture the pair is the path of Definition 1 pinned at $Z(1) = 0$.

Theorem 5 (The cyclic shift)**.** For $\rho \in (-1,1)$, θ_1 is uniform on $[0,1)$ and independent of D.

Proof. For $c \in [0,1)$ let $B_i^c(v) = B_i((c+v) \bmod 1) - B_i(c)$. One shifted bridge is again a bridge [21]; writing $B_2 = \rho B_1 + \bar{\rho} B'$ with B' independent, linearity gives $B_2^c = \rho B_1^c + \bar{\rho} B'^c$, so the pair keeps its law. Subtracting a constant does not move a maximum, so $\theta_i(B^c) = (\theta_i - c) \bmod 1$ and $D(B^c) = D(B)$. With U uniform and independent, $(\theta_1(B^U), D(B^U))$ has the law of (θ_1, D), while $\theta_1(B^U) = (\theta_1 - U) \bmod 1$ is uniform and independent of B, hence of $D(B^U) = D(B)$. □

This is Vervaat's cyclic shift [21] for a pair; it leaves one variable, D, with $\theta_2 = (\theta_1 + D) \bmod 1$.

Theorem 6 (The law of the cyclic gap)**.** For $\rho \in (-1,1)$, D has the density

$$\kappa(u) = \frac{\pi \sin\alpha}{2} \int_0^\infty \int_0^\infty K_u(r_1, r_2)\, K_{1-u}(r_1, r_2)\, dr_1\, dr_2, \qquad 0 < u < 1,$$

with $\kappa(u) = \kappa(1-u)$ and $\kappa \equiv 1$ at $\rho = 0$. As $u \downarrow 0$, and so as $u \uparrow 1$, $\kappa(u) \sim C_{\mathrm{br}} u^{p-2}$ with $C_{\mathrm{br}} = p^3 \sin\alpha\, I_\alpha/(2^p\Gamma(p+1))$, I_α as in Proposition 2. Moreover

$$\operatorname{corr}(\theta_1, \theta_2) = 6E[D^2] - 2 = 6\operatorname{Var} D - \frac{1}{2}.$$

Proof. Follow Theorem 1 for the path pinned at $Z(1) = 0$: the last piece now runs from P_2 back to z_a in time $1-t$, so $\partial_{n_2} S_{1-t}(P_2)$ becomes $\partial_{n_2} p_{1-t}(P_2, z_a)$, and pinning divides by $g_1(0) = 1/(2\pi)$. Integrating over the gaps and over the apex ($da_1\, da_2 = \sin\alpha\, dA(z)$), Chapman–Kolmogorov and Lemma 4(i) give

$$\int_C \partial_{n_1} p_s(P_1, z)\, \partial_{n_2} p_{1-t}(z, P_2)\, dA(z) = \partial_{n_1}\partial_{n_2} p_{1-u}(P_1, P_2) = K_{1-u}(r_1, r_2),$$

$u = t - s$. So on $\{\theta_1 < \theta_2\}$ the density of (θ_1, θ_2) is $2\pi\frac{\sin\alpha}{4}\iint K_u K_{1-u} =: F(u)$, with $F(1-u) = F(u)$, and the mirror half is the same function of $s - t$. Now $D = u$ arises from $\theta_1 < \theta_2$ with $s \in (0, 1-u)$ and from $\theta_2 < \theta_1$ with $\theta_1 - \theta_2 = 1-u$, $s \in (1-u, 1)$, so its density is $(1-u)F(u) + uF(1-u) = F(u)$. At $\rho = 0$ the times are independent and uniform. For the asymptotics, $r_i = \sqrt{u}\, x_i$ and Lemma 2(d) give

$$u^{2-p}\kappa(u) = \frac{\pi \sin\alpha}{2} \iint k(x_1, x_2)\, u^{1-p} K_{1-u}(\sqrt{u}x_1, \sqrt{u}x_2)\, dx_1 dx_2,$$

where the second factor tends to $c_k(x_1x_2)^{p-1}$ (Lemma 2(e)) and is at most $C(x_1x_2)^{p-1}$ (Lemma 4(iii)); the limit is $\frac{\pi\sin\alpha}{2} c_k I_\alpha = C_{\mathrm{br}}$. Finally, by Theorem 5, given $D = d$, θ_1 is uniform and $\theta_2 = \theta_1 + d$ or $\theta_1 + d - 1$, so $E[\theta_1\theta_2 \mid D = d] = \frac{1}{3} - \frac{d}{2} + \frac{d^2}{2}$; with $ED = \frac{1}{2}$ and $\operatorname{Var}\theta_i = \frac{1}{12}$, $\operatorname{cov}(\theta_1, \theta_2) = \frac{1}{2}E[D^2] - \frac{1}{6}$. □

The proof inherits the step of Remark 1. On the circle there is no corner: κ vanishes or blows up at both ends with the diagonal exponent $p - 2$.

Proposition 3 (Elementary closed forms for dihedral wedges)**.** Let $\alpha = \pi/n$, $n \geq 2$, and for $g \in \mathcal{D}_n$ let Σ_g be the matrix of the quadratic form $(x, y) \mapsto |ye_\alpha - xge_0|^2$. Then $\kappa(u)$ is a finite sum over $(g, h) \in \mathcal{D}_n^2$ of polynomials in $1/u$ and $1/(1-u)$ times quadrant moments

$$Q_{a,b}(\Sigma) = \int_0^\infty \int_0^\infty x^a y^b e^{-\frac{1}{2}(x,y)\Sigma(x,y)^\top} dx\, dy,$$
$$\Sigma = \frac{\Sigma_g}{u} + \frac{\Sigma_h}{1-u}, \quad a + b \in \{0, 2, 4\}.$$

With $k = (a+b+2)/2$, $\sigma_1 = \Sigma_{11}$, $\sigma_{12} = \Sigma_{12}$, $\sigma_2 = \Sigma_{22}$, $q(t) = \sigma_1 + 2\sigma_{12}t + \sigma_2 t^2$ and $\Delta = \sigma_1\sigma_2 - \sigma_{12}^2$,

$$Q_{a,b}(\Sigma) = \Gamma(k)\, 2^{k-1} J(b, k), \qquad J(b, k) = \int_0^\infty t^b q(t)^{-k}\, dt,$$

and for $\Delta > 0$: $J(0, 1) = \operatorname{atan2}(\sqrt{\Delta}, \sigma_{12})/\sqrt{\Delta}$,

$$J(0, k+1) = [-\sigma_{12}\sigma_1^{-k} + (2k-1)\sigma_2 J(0, k)]/(2k\Delta),$$

$J(1,k) = [\sigma_1^{1-k}/(2(k-1)) - \sigma_{12}J(0,k)]/\sigma_2$ for $k \geq 2$, and

$$J(b,k) = [J(b-2,k-1) - 2\sigma_{12}J(b-1,k) - \sigma_1 J(b-2,k)]/\sigma_2$$

for $b \geq 2$. The only degenerate case, $\Delta = 0$, occurs for odd n when $ge_0 = he_0 = -e_\alpha$; then all entries of Σ equal some $c > 0$ and $Q_{a,b} = B(a+1,b+1)\Gamma(k)2^{k-1}c^{-k}$. So κ is explicit in rational functions of u, square roots and arctangents.

Proof. By Theorem 4(iii) and Lemma 2(d), $K_u(r_1,r_2)$ is a sum over g of $\operatorname{sgn}(g)/(2\pi u)$ *times $[c_g/u - r^\top S_g r/u^2]\, e^{-r^\top \Sigma_g r/(2u)}$, $r = (r_1,r_2)$, $c_g = n_2 \cdot gn_1$, with S_g the matrix of $(w\cdot n_2)(w\cdot gn_1)$. So $K_u K_{1-u}$ is a double sum of polynomials of degrees 0, 2, 4 times $e^{-r^\top \Sigma r/2}$. In $Q_{a,b}$ put $y = tx$; then $\int_0^\infty x^{2k-1}e^{-x^2 q(t)/2}dx = \Gamma(k)2^{k-1}q(t)^{-k}$. $J(0,1)$ is elementary. From $(\sigma_2 t + \sigma_{12})^2 = \sigma_2 q - \Delta$,*

$$\frac{d}{dt}[(\sigma_2 t + \sigma_{12})q^{-k}] = (1-2k)\sigma_2 q^{-k} + 2k\Delta q^{-k-1},$$

whose integral is $-\sigma_{12}\sigma_1^{-k}$: the recursion. Writing $t = [(\sigma_2 t + \sigma_{12}) - \sigma_{12}]/\sigma_2$ gives $J(1,k)$, and $t^2 = (q - 2\sigma_{12}t - \sigma_1)/\sigma_2$ the reduction in b; all integrals converge since $b \leq 2k-2$. Σ is singular only if Σ_g and Σ_h are, with a common kernel, and Σ_g is singular exactly when $ge_0 = \pm e_\alpha$. As ge_0 lies at an angle in $2\pi\mathbb{Z}/n$, $ge_0 = e_\alpha$ never occurs and $ge_0 = -e_\alpha$ occurs if and only if n is odd; the form is then $(x+y)^2$, and $x = R\tau$, $y = R(1-\tau)$ gives the Beta integral. □

Corollary 4 (Chaos structure and the antithetic endpoint for bridges)**.** For the bridges of Definition 3, $\operatorname{corr}(\theta_1,\theta_2) = \sum_{n\geq 1} c_n^{\mathrm{br}}\rho^n$ with $c_n^{\mathrm{br}} \geq 0$, $\sum_n c_n^{\mathrm{br}} = 1$ and $\sum_n (-1)^n c_n^{\mathrm{br}} = -(\pi^2-9)/3$.

Proof. $B_i = W_i - vW_i(1)$ is linear in W_i, and $W_2 = \rho W_1 + \bar\rho W'$ gives $B_2 = \rho B_1 + \bar\rho B'$; so the proof of Theorem 2 applies to $\theta(B) - \frac12$, with $\operatorname{Var}\theta = \frac{1}{12}$. At $\rho = -1$ the covariance of the times of the maximum and minimum of a bridge is $-(\pi^2-9)/36$ [13]; dividing by $\frac{1}{12}$ gives the correlation. □

So the covariance at $\rho = -1$ is -0.024156 and the correlation -0.289868.

Method. Algorithm 1 with the path pinned at $Z(1) = 0$. Theorem 5: chi-square tests of uniformity of θ_1 and of independence on a 10×10 table of (θ_1, D). Theorem 6: the integral of κ, $\kappa \equiv 1$ at $\rho = 0$, the histogram of D, the correlation against $6E[D^2]-2$, the exponent (Table 2) and C_{br}. Proposition 3: its closed form against quadratures of κ through the image kernels and through the series. Corollary 4: the covariance extrapolated to $\rho = -1$.

Parameters. $\rho = -0.9$, $-\sqrt{3}/2$, $-1/\sqrt{2}$, -0.5, 0, 0.5, 0.9; three seeds of 200,000 pairs, $n = 1000$; the closed form at $n = 2$, 3, 4, 6. Tolerances: chi-square $p \geq 10^{-4}$, $|z| \leq 4$, 10^{-5} for the integral, 10^{-7} relative for the closed form.

Result. The smallest p-values are 0.068 (uniformity), 0.0596 (independence) and 0.250 (law of D). The integral of κ is 1 within 4.1×10^{-6}, and $\kappa = 1$ at $\rho = 0$ within 7.4×10^{-15}. The simulated correlation agrees with $6E[D^2]-2$ within 0.79 standard errors (Table 5).

$u^{2-p}\kappa(u)$ at $u = 10^{-5}$ against C_{br}: $\rho = -0.5$: 9.34897 against 9.34932; $\rho = 0.3$: 0.48006 against 0.48005; $\rho = 0.5$: 0.30786 against 0.30786; $\rho = 0.7$: 0.18810 against 0.18810; $\rho = 0.9$: 0.08624 against 0.08624; $\rho = 0.99$: 0.02365 against 0.02365. The closed form agrees with both quadratures within a relative 4.6×10^{-11}, its quadrant moments with numerical integration within 6.7×10^{-16}. The extrapolated covariance at $\rho = -1$ is -0.024156, against $-(\pi^2 - 9)/36 = -0.024156$, a difference of 3.7×10^{-7}.

Error. All simulated tests pass with $|z| \le 0.79$; C_{br} agrees within a relative 3.8×10^{-5}.

Source. Quadrature of Theorem 6 for $E[D^2]$, and Algorithm 1 for bridges with 600,000 pairs per correlation; `numbers.json`, `derive.py`.

Columns. The correlation; the mean square cyclic gap from κ; the correlation of the times from Theorem 6; the simulated correlation.

Table 5: The correlation of the times of the maxima of correlated Brownian bridges, from the law of the cyclic gap and by simulation.

ρ	$E[D^2]$	$6E[D^2] - 2$ **(Theorem 6)**	**Monte Carlo**
-0.9	0.288895	-0.26663	-0.26724
$-\sqrt{3}/2$	0.290247	-0.25852	-0.25773
$-1/\sqrt{2}$	0.296827	-0.21904	-0.21850
-0.5	0.306132	-0.16321	-0.16371
0	0.333333	0	-0.00112
$+0.5$	0.373084	0.23850	0.23765
$+0.9$	0.436337	0.61802	0.61761

Script. `fig_bridge.py`: κ for five correlations, the closed form at $\rho = -1/2$ as white dashes, and the simulated histograms of D, from `results.npz`.

Shows. Theorems 5 and 6 and Proposition 3.

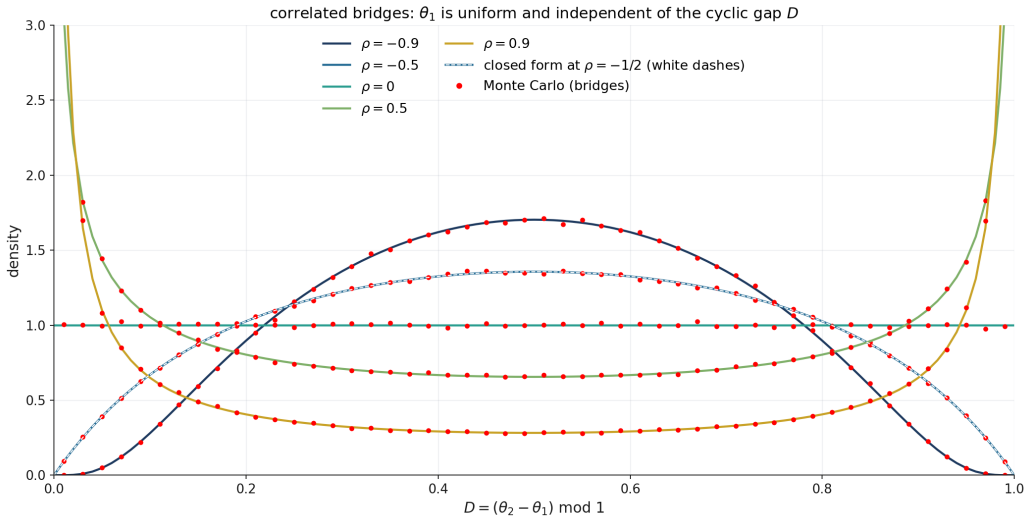


Figure 6: The density of the cyclic gap between the times of the maxima of two correlated Brownian bridges for correlations minus nine tenths, minus one half, zero, one half and nine tenths, symmetric about one half, with the elementary closed form at minus one half as white dashes and simulated histograms as dots.

A hump for $\rho < 0$, flat at $\rho = 0$, a bowl for $\rho > 0$.

8. Several Motions

Remark 4 (The decomposition for N motions). For N motions $W_i = \langle u_i, Z \rangle$ the event $\{M_i < a_i \text{ for all } i\}$ keeps Z in a polyhedral cone whose facet i is touched at θ_i. Formally the argument of Theorem 1 cuts the path into a first exit, $N-1$ facet-to-facet passages in the order of the times, and a survival; for pairwise correlations $-\cos(\pi/m_{ij})$ the cone is a Weyl chamber and each kernel an alternating Gaussian sum [20]. But facets are $(N-1)$-dimensional, and for $N = 3$ the density is already a four-fold Gaussian integral over a polyhedral cone, which we have not reduced. Section 8 is numerical.

Method. Algorithm 1 extended to N motions $W = AZ$, Z a standard Brownian motion in $\mathbb{R}^d$ and A with rows of unit length, records all argmax times. Each pair is compared with the two-motion law through its correlation, and the orderings of the times are counted. Numerical only.

Parameters. The chain A_3: $W_i = (B_{i+1} - B_i)/\sqrt{2}$, $i = 1, 2, 3$, B_j independent, so neighbors have correlation $-1/2$ and W_1, W_3 are independent (a Weyl chamber); the chain A_4, built the same way; equicorrelated triples at $\rho = 0.5$ and -0.4 (not Weyl chambers). Three seeds of 200,000 paths each, $n = 1000$; $|z| \leq 4$ per pair.

Result. All 15 pairwise correlations agree with the two-motion law within 2.11 standard errors (Table 6). With labels listing the motions in increasing order of their argmax times, the six orderings in A_3 have probabilities 132: 0.1820, 231: 0.1817, 213: 0.1815, 312: 0.1814, 321: 0.1367, 123: 0.1367; the two orders in which the middle motion's maximum lies between its neighbors' have total 0.2734 instead of 1/3. In A_4 the alternating 3142

(0.0669) and 2413 (0.0668) lead, against $1/24 = 0.0417$, and the monotone 1234 and 4321 trail (0.0215, 0.0213). The equicorrelated orderings lie in $[0.1660, 0.1674]$ at $\rho = 0.5$ and $[0.1662, 0.1675]$ at $\rho = -0.4$, against $1/6 = 0.1667$.

Error. Pairs deviate from the two-motion law by at most 2.11 standard errors; the departures of the chains from exchangeability are far beyond the binomial error near 1/6 over 600,000 paths, 0.00048.

Source. Algorithm 1 for $N = 3$ and 4 motions, 600,000 paths per configuration in three seeds; the two-motion curve of Section 5; `numbers.json`, `derive.py`.

Columns. The configuration; the number of pairs with correlation ρ_{ij}; the range of the simulated correlations of their argmax times; the two-motion value at ρ_{ij}; the simulated mean of the product of all argmax times.

Table 6: Pairwise correlations of the argmax times of several correlated motions, by simulation, against the two-motion law.

configuration	**pairs**	ρ_{ij}	$\mathrm{corr}(\theta_i, \theta_j)$, **Monte Carlo**	**two-motion value**	$E[\prod_i \theta_i]$
A_3 chain	2	-0.5	-0.2965 to -0.2939	-0.2953	0.08783
	1	0	-0.0023	0	
A_4 chain	3	-0.5	-0.2964 to -0.2949	-0.2953	0.03618
	3	0	+0.0002 to +0.0019	0	
equicorrelated	3	+0.5	+0.3278 to +0.3295	+0.3277	0.18665
equicorrelated	3	-0.4	-0.2381 to -0.2351	-0.2365	0.08067

9. Random Walks

Definition 4 (Correlated walks and their argmax indices)**.** Let $\xi_k = (\xi_k^{(1)}, \xi_k^{(2)})$, $1 \le k \le n$, be i.i.d. with centered coordinates of unit variance and correlation ρ, $S_k = \xi_1 + \cdots + \xi_k$, $S_0 = 0$, and ϑ_i the first index at which $S_k^{(i)}$, $0 \le k \le n$, is maximal. The four step laws are: Gaussian; the mix $(X, \rho X + \bar{\rho} Y)$ with X, Y i.i.d. uniform on $(-\sqrt{3}, \sqrt{3})$; the same with Laplace variables of unit variance; and copy-or-fresh, with $\xi^{(1)}$ Gaussian and $\xi^{(2)} = \mathrm{sign}(\rho)\xi^{(1)}$ with probability $|\rho|$, an independent Gaussian otherwise.

Each coordinate is a walk with a continuous symmetric step law; copy-or-fresh is singular in the plane. By the invariance principle [26] and the continuity of the argmax at paths with one maximum, $(\vartheta_1, \vartheta_2)/n$ converges in law to (θ_1, θ_2).

Remark 5 (What is universal and what is not). $P(\vartheta_i = 0) = P(S_1^{(i)} \le 0, \dots, S_n^{(i)} \le 0) = \binom{2n}{n} 4^{-n}$ for every symmetric continuous step law [22]: the marginal is universal. $P(\vartheta_1 = \vartheta_2 = 0)$ is the probability that the planar walk stays in a cone for n steps, whose exponent $\pi/(2\alpha)$ is universal but whose constant depends on the step law [17]. A coincidence $\vartheta_1 = \vartheta_2$ corresponds heuristically to $|\theta_1 - \theta_2| \lesssim 1/n$, of probability of order

$n^{-\pi/(2\alpha)}$ for $\rho < 0$ and $n^{-(\pi/\alpha-1)}$ for $\rho > 0$ by Corollary 2; this is a heuristic, which Section 9 tests.

Method. For the four laws of Definition 4 at $\rho = \pm 0.5$ and $n = 10$, 100, 1000 we record $(\vartheta_1, \vartheta_2)$ and ask: does $P(\vartheta_1 = 0)$ match $\binom{2n}{n}4^{-n}$ for every law; do the frequencies of $\vartheta_1 = \vartheta_2 = 0$ differ between laws by more than 10 standard errors; does the correlation converge to the Brownian value; does $P(\vartheta_1 = \vartheta_2)$ decay with the order of Remark 5? All numerical.

Parameters. 12,000,000 paths at $n = 10$, 1,200,000 at $n = 100$, 300,000 at $n = 1000$, per law and correlation, in three seeds; standard errors from 30 batches. Tolerances: $|z| \leq 4$ for the marginal and the limit, $|z| \geq 10$ to declare non-universality.

Result. $P(\vartheta_1 = 0)$ agrees with Sparre Andersen's value within 2.24 standard errors in all 24 cases. The largest pairwise $|z|$ between laws for $P(\vartheta_1 = \vartheta_2 = 0)$ is, at $\rho = -0.5$, $n = 10$: 26.3; $n = 100$: 2.2, and at $\rho = +0.5$, $n = 10$: 93.3; $n = 100$: 10.2. At $n = 1000$ the correlation agrees with the Brownian value for every law within 1.67 standard errors (Figure 7). The observed orders of $P(\vartheta_1 = \vartheta_2)$ between $n = 100$ and 1000 are within 0.087 of Remark 5 (Table 7), the largest deviation for copy-or-fresh at $\rho = -0.5$.

Error. Universality of the marginal holds within 2.24 and convergence within 1.67 standard errors; the joint law is law-dependent at up to 93.3. At $n = 100$, $\rho = -0.5$, the differences are within noise, so we claim non-universality only where detected.

Source. Simulated walks with 12,000,000 paths at $n = 10$, 1,200,000 at $n = 100$ and 300,000 at $n = 1000$ per law and correlation; `numbers.json`, `derive.py`.

Columns. The step law; the correlation; the frequency of $\vartheta_1 = \vartheta_2 = 0$ at $n = 10$; the correlation of the two indices at $n = 10$ and $n = 1000$, with standard errors from 30 batches; the observed order of $P(\vartheta_1 = \vartheta_2)$ in n, from $n = 100$ to $n = 1000$; the order of Remark 5, $-\pi/(2\alpha)$ for $\rho < 0$ and $-(\pi/\alpha - 1)$ for $\rho > 0$.

Table 7: Indices of the maxima of two correlated random walks for four step laws with the same correlation.

step law	ρ	$P(\vartheta_1 = \vartheta_2 = 0)$, $n = 10$	**corr,** $n = 10$	**corr,** $n = 1000$	**order of** $P(\vartheta_1 = \vartheta_2)$	**predicted**
Gaussian	-0.5	0.007937	-0.2949 ± 0.0003	-0.2943 ± 0.0016	-1.530	-1.500
Gaussian	$+0.5$	0.068857	$+0.3278 \pm 0.0003$	$+0.3312 \pm 0.0021$	-0.480	-0.500
uniform mix	-0.5	0.008382	-0.2976 ± 0.0002	-0.2952 ± 0.0014	-1.563	-1.500
uniform mix	$+0.5$	0.066495	$+0.3224 \pm 0.0003$	$+0.3251 \pm 0.0016$	-0.481	-0.500
Laplace mix	-0.5	0.007949	-0.2896 ± 0.0003	-0.2933 ± 0.0015	-1.544	-1.500
Laplace mix	$+0.5$	0.070970	$+0.3362 \pm 0.0003$	$+0.3273 \pm 0.0018$	-0.479	-0.500
copy-or-fresh	-0.5	0.008917	-0.2911 ± 0.0003	-0.2931 ± 0.0013	-1.413	-1.500
copy-or-fresh	$+0.5$	0.076303	$+0.3556 \pm 0.0003$	$+0.3283 \pm 0.0025$	-0.475	-0.500

Script. `fig_walks.py`: the correlation of the two indices against n for the four step laws, with bars of two standard errors and the Brownian value, from `numbers.json`; logarithmic horizontal axis.

Shows. Section 9.

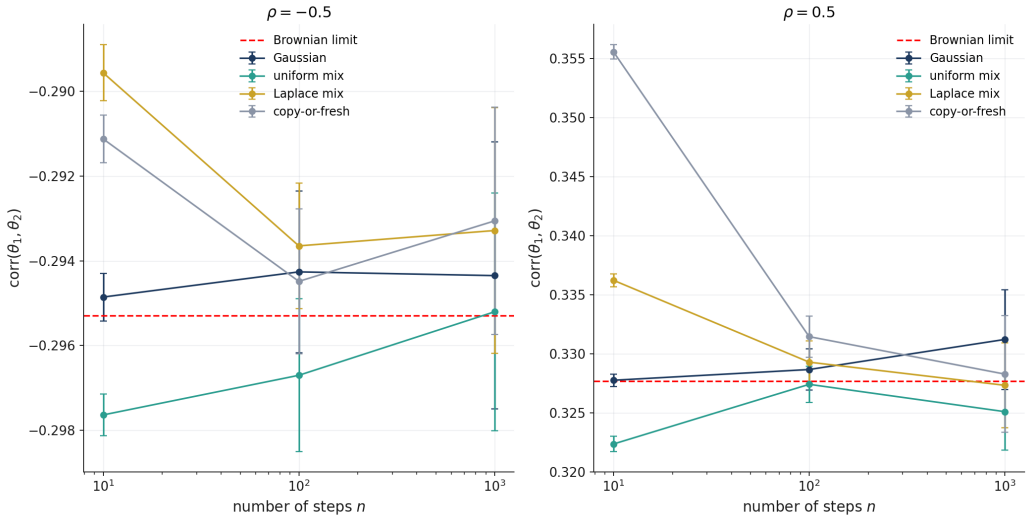


Figure 7: The correlation of the indices of the maxima of two correlated random walks against the number of steps, ten, one hundred and one thousand, for Gaussian, uniform-mix, Laplace-mix and copy-or-fresh steps at correlations minus one half and one half, converging to the Brownian value drawn as a dashed line.

The laws differ at $n = 10$ and meet the Brownian value at $n = 1000$.

10. Limits

Remark 6 (What is not proved). (a) In Theorems 1 and 6 the step of Remark 1 is argued at the level of densities. (b) $\operatorname{corr}(\theta_1, \theta_2)$ has no known closed form at any $\rho \neq 0$ in $(-1, 1)$: it is a moment of a double integral of Bessel series, or a chaos series with only c_1 and two sums exact. (c) The behavior near $\rho = 1$, the decay $c_n \sim n^{-3/2}$ and $|\operatorname{corr}(\theta_1, \theta_2)| < |\operatorname{corr}(M_1, M_2)|$ are observations (Remark 2). (d) An elementary f_ρ at $\alpha = \pi/n$ is not derived (Remark 3). (e) Sections 8 and 9 are numerical, and the decay of walk coincidences rests on a heuristic (Remark 5).

The value of [4] is reproduced from the wedge series only for $|\rho| \leq 0.9$, at $\rho = 0.99$ by simulation alone. Within a refined sub-step of Algorithm 1 the two maxima are drawn independently given the endpoints, and gaps below the sub-step scale, which at $\rho = 0.99$ carry a noticeable share of the mass, are resolved by the formula only. Novelty is claimed to our knowledge only.

11. Conclusion

Two correlated Brownian motions are one planar path in a wedge of angle $\alpha = \arccos(-\rho)$ whose apex is the pair of maxima, and the path touches the two edges at the two argmax times. Cutting it there gives the joint density of (θ_1, θ_2) through two Bessel series of the wedge heat kernel, an exact identity for the probability that both maxima occur before t, and explicit local exponents: the two times repel each other for $\rho < 0$ and attract each other for $\rho > 0$, the argmax counterpart of the first-passage dichotomy of Kou and Zhong. The correlation of the times is a power series in ρ with non-negative coefficients, total 1, alternating sum $(6 - 7\zeta(3))/4$ and first coefficient $4 - 32/(3\pi)$; it has no closed form, but these values bound it on both sides. At $\alpha = \pi/n$ the kernels are finite image sums, and for correlated bridges the first time is uniform and independent of the cyclic gap, whose law is elementary at $\alpha = \pi/n$. For three or four motions and for random walks the findings are numerical. Open are a proof of the planar decomposition step at full rigor, the asymptotics of the chaos coefficients, an elementary density at $\alpha = \pi/n$, and the joint law for three or more motions.

References

[1] Shepp, L. A. (1979). The joint density of the maximum and its location for a Wiener process with drift. *Journal of Applied Probability*. https://doi.org/10.2307/3212910

[2] Denisov, I. V. (1984). A random walk and a Wiener process near a maximum. *Theory of Probability and Its Applications*. https://doi.org/10.1137/1128082

[3] Majumdar, S. N., Randon-Furling, J., Kearney, M. J., & Yor, M. (2008). On the time to reach maximum for a variety of constrained Brownian motions. *Journal of Physics A: Mathematical and Theoretical*. https://doi.org/10.1088/1751-8113/41/36/365005

[4] Rogers, L. C. G., & Shepp, L. (2006). The correlation of the maxima of correlated Brownian motions. *Journal of Applied Probability*. https://doi.org/10.1239/jap/1158784954

[5] Iyengar, S. (1985). Hitting lines with two-dimensional Brownian motion. *SIAM Journal on Applied Mathematics*. https://doi.org/10.1137/0145060

[6] Shao, J., & Wang, X. (2013). Estimates of the exit probability for two correlated Brownian motions. *Advances in Applied Probability*. https://doi.org/10.1239/aap/1363354102

[7] Dębicki, K., Ji, L., & Rolski, T. (2020). Exact asymptotics of component-wise extrema of two-dimensional Brownian motion. *Extremes*. https://doi.org/10.1007/s10687-020-00387-y

[8] Spitzer, F. (1958). Some theorems concerning 2-dimensional Brownian motion. *Transactions of the American Mathematical Society*. https://doi.org/10.1090/S0002-9947-1958-0104296-5

[9] Bañuelos, R., & Smits, R. G. (1997). Brownian motion in cones. *Probability Theory and Related Fields*. https://doi.org/10.1007/s004400050111

[10] Metzler, A. (2010). On the first passage problem for correlated Brownian motion. *Statistics & Probability Letters*. https://doi.org/10.1016/j.spl.2009.11.001

[11] Kou, S., & Zhong, H. (2016). First-passage times of two-dimensional Brownian motion. *Advances in Applied Probability*. https://doi.org/10.1017/apr.2016.64

[12] Mori, F., Majumdar, S. N., & Schehr, G. (2019). Time between the maximum and the minimum of a stochastic process. *Physical Review Letters*. https://doi.org/10.1103/PhysRevLett.123.200201

[13] Mori, F., Majumdar, S. N., & Schehr, G. (2020). Distribution of the time between maximum and minimum of random walks. *Physical Review E*. https://doi.org/10.1103/PhysRevE.101.052111

[14] Hartmann, A. K., & Majumdar, S. N. (2025). Exact joint distributions of three global characteristic times for Brownian motion. *Physical Review E*. https://doi.org/10.1103/PhysRevE.111.044134

[15] Houdré, C., & Litherland, T. J. (2017). On a generalization of the arcsine law. *arXiv preprint*. arXiv:1710.04559

[16] Varadhan, S. R. S., & Williams, R. J. (1985). Brownian motion in a wedge with oblique reflection. *Communications on Pure and Applied Mathematics*. https://doi.org/10.1002/cpa.3160380405

[17] Denisov, D., & Wachtel, V. (2015). Random walks in cones. *The Annals of Probability*. https://doi.org/10.1214/13-AOP867

[18] Gebelein, H. (1941). Das statistische Problem der Korrelation als Variations- und Eigenwertproblem und sein Zusammenhang mit der Ausgleichsrechnung. *Zeitschrift für Angewandte Mathematik und Mechanik*. https://doi.org/10.1002/zamm.19410210604

[19] Nualart, D. (2006). *The Malliavin Calculus and Related Topics*. Springer. https://doi.org/10.1007/3-540-28329-3

[20] Karlin, S., & McGregor, J. (1959). Coincidence probabilities. *Pacific Journal of Mathematics*. https://doi.org/10.2140/pjm.1959.9.1141

[21] Vervaat, W. (1979). A relation between Brownian bridge and Brownian excursion. *The Annals of Probability*. https://doi.org/10.1214/aop/1176995155

[22] Sparre Andersen, E. (1954). On the fluctuations of sums of random variables II. *Mathematica Scandinavica*. https://doi.org/10.7146/math.scand.a-10407

[23] Borodin, A. N., & Salminen, P. (2002). *Handbook of Brownian Motion: Facts and Formulae*. Birkhäuser. https://doi.org/10.1007/978-3-0348-8163-0

[24] Beskos, A., Papaspiliopoulos, O., & Roberts, G. O. (2006). Retrospective exact simulation of diffusion sample paths with applications. *Bernoulli*. https://doi.org/10.3150/bj/1165269151

[25] Watson, G. N. (1995). *A Treatise on the Theory of Bessel Functions*. Cambridge University Press.

[26] Billingsley, P. (1999). *Convergence of Probability Measures*. Wiley. https://doi.org/10.1002/9780470316962

Zamrik Quant Research
The research arm of Zamrik Quant Lab

About the Desk

Stochastic Analysis Desk

Zamrik Quant Research

How random processes behave — Itô calculus, diffusions, local time, Fokker–Planck — in theory and in application.

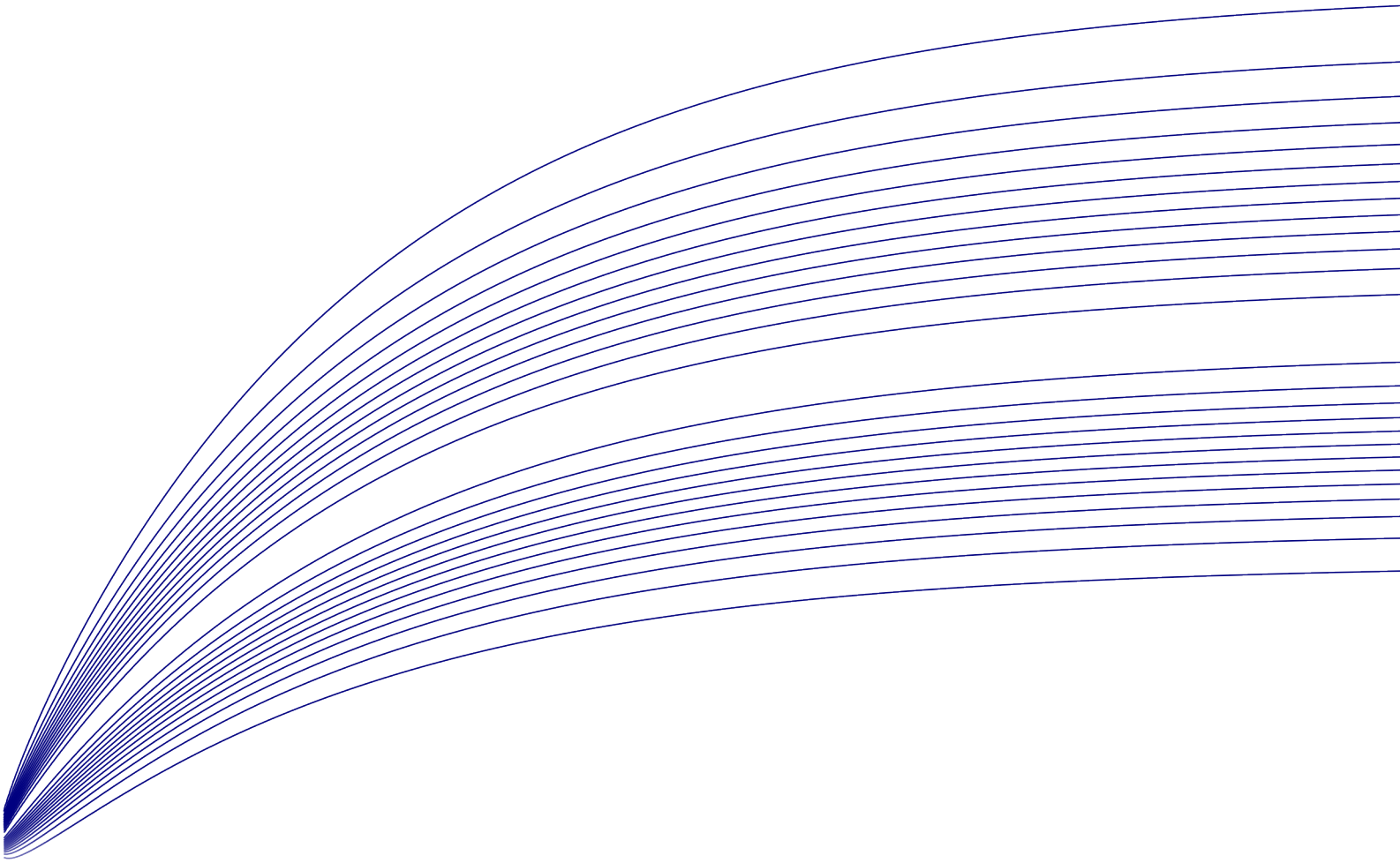
Stochastic analysis is the grammar of every other desk: a price, an order queue, a population or a value function is a functional of a random path, and what can be said about it depends on what can be proved about the path. The Stochastic Analysis desk works on those proofs and on the exact formulas they produce.

Its core questions are the classical ones, asked with care: when a diffusion first reaches a boundary, fixed or moving; how long it spends at each level before it does; and what happens at the boundary itself — reflection, killing, a sticky or skewed point, a reset to the start. The answers come through Itô calculus and martingale methods, local time and Tanaka's formula, Ray–Knight theorems, time changes, and the Feynman–Kac and Fokker–Planck equations that turn questions about paths into equations for expectations and densities. Wherever the problem allows, the desk derives the law in closed form and then checks it against an independently built simulation.

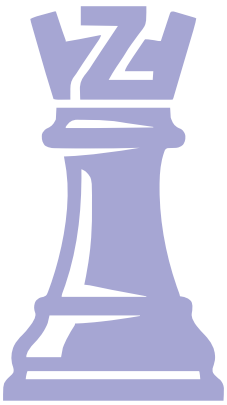
The results travel. The same calculus corrects a barrier that is checked once a day, explains why most stocks lose to the average stock, separates real correlation from the noise of random matrices, sets the acceptance rate of a Metropolis sampler, and models a neuron's membrane and a day's rainfall. The desk also studies the numerics that decide whether a simulated path tells the truth: the strong and weak convergence of Euler–Maruyama and Milstein schemes, Brownian-bridge corrections for barriers monitored in discrete time, and the error left when a continuous process is sampled on a grid.

The desk is supervised by **Dr. T. Zamrik**, Head of Zamrik Quant Research, PhD, Imperial College London (2011).

Notes



Fokker–Planck density of the Cox–Ingersoll–Ross process: $\partial_t p = -\partial_x[\kappa(\theta - x)\,p] + \frac{1}{2}\sigma^2 \partial_{xx}(x\,p)$



ZAMRIK QUANT RESEARCH

The research arm of Zamrik Quant Lab



WP-2025-19558953
zamrik.com